SANDIA REPORT
SAND99-0164
Unlimited Release
Printed July 2000

STAMMT-R
Solute Transport and Multirate Mass Transfer in Radial Coordinates

A FORTRAN code for modeling and analyzing radial single-well and two-well tracer tests in formations exhibiting multiples rates of diffusive mass transfer

VERSION 1.01

Roy Haggerty, Sean W. Fleming, Sean A. McKenna

Prepared by
Sandia National Laboratories
Albuquerque, New Mexico 87185 and Livermore, California 94550

Sandia is a multiprogram laboratory operated by Sandia Corporation, a Lockheed Martin Company, for the United States Department of Energy under Contract DE-AC04-94AL85000.

Sandia National Laboratories

Issued by Sandia National Laboratories, operated for the United States Department of Energy by Sandia Corporation.

Available to DOE and DOE contractors from
Office of Scientific and Technical Information
P.O. Box 62
Oak Ridge, TN 37831

Prices available from (703) 605-6000
Web site: http://www.ntis.gov/ordering.htm

Available to the public from
National Technical Information Service
U.S. Department of Commerce
5285 Port Royal Rd
Springfield, VA 22161

NTIS price codes
Printed copy: A04
Microfiche copy: A01

SAND99–0164
Unlimited Release
Printed July 2000

STAMMT–R
Solute Transport and Multirate Mass Transfer in Radial Coordinates

A FORTRAN code for modeling and analyzing radial single–well and two–well tracer tests in formations exhibiting multiple rates of diffusive mass transfer

VERSION 1.01

Roy Haggerty, Sean W. Fleming
Department of Geosciences
104 Wilkinson Hall
Oregon State University
Corvallis, OR 97331–5506

Sean A. McKenna
Geohydrology Department
Sandia National Laboratories
P.O. Box 5800
Albuquerque, NM 87185–0735

Abstract

STAMMT-R is a FORTRAN 77 code that solves the advective-dispersive and rate-limited mass transfer equations for solute transport in groundwater in radial coordinates. STAMMT-R is unique in that rate-limited mass transfer can be modeled as heterogeneous at the pore-scale. Heterogeneous rate-limited mass transfer is diffusion concurrently into and out of a distribution of immobile zones, which may include matrix blocks of varying sizes or geologic materials with differing diffusion characteristics.

STAMMT-R solves the governing equations in one of two modes: (1) forward simulation, where parameters are specified and concentrations are calculated over time and space; or (2) parameter estimation, where concentration data are provided by the user and the best-fit parameters are calculated from the data. It should be noted that the test problems shown in this manual are used only to verify the forward simulation mode. The model can be used for two different flow conditions: (1) single-well injection-withdrawal (SWIW, or "push-pull") where a solute and chaser are injected into an aquifer, followed by a resting period, and then the solute is pumped out of the aquifer at the same well; or (2) two-well injection-withdrawal, where a solute and chaser are injected into an aquifer at one well, then pumped out of the aquifer at a second well. Mass transfer options available in STAMMT-R are (1) a lognormal distribution of layered diffusion rate coefficients (D_d/a^2); (2) conventional matrix diffusion into spherical immobile zones (single rate, double-porosity model); or (3) a non-parametric distribution of first-order rate coefficients. The latter option includes conventional first-order mass transfer as its simplest form. In either forward simulation or parameter estimation mode, STAMMT-R can simulate both flow conditions (SWIW and two-well) simultaneously with the same parameter set. Solution of the flow and transport equations is analytic in the Laplace-domain, and the solution is inverted to the time-domain using a numerical algorithm.

The following general assumptions have been invoked in developing STAMMT-R: (1) velocities within the formation are constant in time with the exception of specified changes due to pumping; (2) all parameters are homogeneous in space; (3) there is no regional gradient; (4) rate-limited mass transfer is dominated by diffusive processes; (5) if diffusional mass transfer is used, the layered diffusion rate coefficient, D_d/a^2, is assumed to have either a lognormal distribution or is single-valued (conventional spherical matrix diffusion). The main limitations of the code beyond the assumptions listed above are the following (see Section 6 for details): (1) chaser (tracer-free) injection must have non-zero volume; (2) the code is inaccurate for single-rate diffusion with large block sizes at early time; and (3) the code is moderately calculation-intensive, resulting in forward run times in excess of 5 minutes on a 266 MHz Pentium II and much longer parameter estimation run times.

Compilation of version 1.0 requires a FORTRAN 77 compiler with access to IMSL (International Mathematical and Statistical Libraries) Version 3.0.

Reference as: Haggerty, R., S. W. Fleming, and S. A. McKenna, *STAMMT-R: Solute Transport and Multirate Mass Transfer in Radial Coordinates, Version 1.01*, SAND99-0164, Sandia National Laboratories, Albuquerque, New Mexico, 1999.

Acknowledgments

Funding for this work was provided to R. Haggerty by Sandia National Laboratories under contract AQ-6866. The content of the code and of the user manual do not necessarily represent the views of Sandia National Laboratories nor of the US Department of Energy. We are very thankful to Lucy Meigs, Michael Kelley, Susan Altman, Yvonne Tsang, Toya Jones, Charles Tilburg, and Joanna Ogintz for their assistance in preparing the code and manual, reviewing the manual, and for running many simulations to check the code's output and accuracy. We thank Ron Dykhuizen and Michael Gross for their helpful reviews, and Jim Ramsey for reviewing the document and code several times at different stages in its development.

Table of Contents

1. Introduction

Understanding and predicting mass transfer coupled with solute transport in porous media is central to a number of problems in nuclear waste disposal, reservoir engineering and hydrocarbon extraction, and groundwater remediation. Mass transfer is the set of processes that control movement of a chemical between mobile (advection dominated) domains and immobile (diffusion or sorption dominated) domains within a porous medium. Transport is dominated by advection in the mobile domain, and by diffusion and/or sorption in the immobile domain. Consequences of mass transfer on solute transport are numerous and may include (1) apparent reduction in average advective velocity through time or space, by as much as several orders of magnitude; (2) long "tails" in concentration histories during removal of a solute from a porous medium; (3) very poor accuracy when taking experimental results from one time or spatial scale and applying them to another scale.

A growing body of research demonstrates that diffusive and sorptive mass transfer are very complex phenomena in natural porous media, and frequently occur over multiple time-scales. *Haggerty and Harvey* [1997] show that mass transfer in many experiments occurs over time-scales varying from minutes to decades. Increasingly, it is recognized that conventional, single-rate, models of mass transfer fail to account for the important effects of geometric and chemical complexity found in natural porous media. Although conventional understanding and modeling of mass transfer are adequate for fitting to experimental data, they provide very poor predictions of solute behavior over time-scales and spatial-scales longer than the experiment. For these reasons, we have developed STAMMT-R.

STAMMT-R is a FORTRAN 77 code that solves the advective-dispersive and rate-limited mass transfer equations for solute transport in groundwater in radial coordinates. STAMMT-R is unique in that rate-limited mass transfer can be modeled as heterogeneous at the pore-scale. Heterogeneous rate-limited mass transfer is diffusion concurrently into and out of a distribution of immobile zones, which may include matrix blocks of varying sizes or geologic materials with differing diffusion characteristics.

STAMMT-R solves the governing equations in one of two modes: (1) forward simulation, where parameters are specified and concentrations are calculated over time and space; or (2) parameter estimation, where concentration data are provided by the user and the best-fit parameters are calculated from the data. It should be noted that the test problems shown in this manual are used only to verify the forward simulation mode. The model can be used for two different flow conditions: (1) single-well injection-withdrawal (SWIW, or "push-pull") where a solute and chaser are injected into an aquifer, followed by a resting period, and then the solute is pumped out of the aquifer at the same well; or (2) two-well injection-withdrawal (hereafter referred to as a two-well test or model), where a solute and chaser are injected into an aquifer at one well, then pumped out of the aquifer at a second well. Mass transfer options available in STAMMT-R are (1) a lognormal distribution of layered diffusion rate coefficients (D_d/a^2); (2) conventional matrix diffusion into spherical immobile zones (single rate, double-porosity model); or (3) a non-parametric distribution of first-order rate coefficients. The latter option includes conventional first-order mass transfer as its simplest form. In either forward simulation

or parameter estimation mode, STAMMT-R can simulate both flow conditions (SWIW and two-well) simultaneously with the same parameter set. Solution of the flow and transport equations is analytic in the Laplace-domain, and the solution is inverted to the time-domain using a numerical algorithm.

The following general assumptions have been invoked in developing STAMMT-R: (1) velocities within the formation are constant in time with the exception of specified changes due to pumping; (2) all parameters are homogeneous in space; (3) there is no regional gradient; (4) rate-limited mass transfer is dominated by diffusive processes; (5) if diffusional mass transfer is used, the layered diffusion rate coefficient, D_d/a^2, is assumed to have either a lognormal distribution or is single-valued (conventional spherical matrix diffusion). The second set of assumptions primarily guarantees that flow is radially symmetric. This is less significant for an SWIW test than for other types of tests, particularly if the first assumption is valid, because the tracer leaves the well and comes back to the well along the same (or very similar) path [*Ostensen*, 1998].

Use of version 1.0 requires that the code be compiled and run on a computer loaded with IMSL (International Mathematical and Statistical Libraries) Version 3.0. See Section 3 for information on IMSL.

2. Theory

2.1. Overview of Multirate Mass Transfer

Rates of mass transfer between zones of mobile and immobile water vary locally in space and correspond in a general but often unknown way to small-scale variations in formation properties. These properties are numerous and include at least the following [*Pedit and Miller*, 1994; *Haggerty and Gorelick*, 1995; *Pignatello and Xing*, 1996]: (1) the types of minerals and their spatial distributions; (2) the geometry, chemistry, and mineralogy of coatings on the surfaces of soil particles; (3) the volume, size, and geometry of macro- or micro-porosity in aquifer particles and aggregates of particles; (4) the external and internal geometry of small clay lenses or other low-permeability material, and the proportions of this material; (5) variations in hydraulic conductivity; (6) the quantity and distribution of organic material; (7) the chemistry of the water and solute. As a consequence, rates of mass transfer may vary tremendously over short distances in the subsurface. Although some of this variability is dependent on sorption properties, mass transfer of nonsorbing solutes is influenced by any property that affects the size, volume, or geometry of the immobile pore spaces. Therefore, it is apparent that we should account for a distribution of diffusion rate coefficients at the small scale, as they affect larger-scale transport; yet the majority of existing models account for only one or two discrete rate coefficients. In addition, the degree of variability in mass transfer processes has not yet been quantified for most natural materials.

Villermaux [1981] first proposed a model that allows for multiple, simultaneous mass transfer into or from immobile zones of different sizes and shapes. Various other authors have proposed similar models that allow for at least two or more simultaneous, rate-limited mass transfer processes [e.g., *Dougharty*, 1972; *Rao et al.*, 1982, *Cooney et al., 1983*; *Neretnieks and Rasmuson*, 1984; *Rasmuson*, 1985; *Wu and Gschwend*, 1988;

Brusseau et al., 1989; *Fong and Mulkey*, 1990; *Valocchi*, 1990; *Lafolie and Hayot*, 1993; *Connaughton et al.*, 1993; *Pedit and Miller*, 1994, 1995; *Chen and Wagenet*, 1995; *Haggerty and Gorelick*, 1995, 1998; *Culver et al.*, 1997; and *Cunningham et al.*, 1997]. *Pedit and Miller* [1994] give a thorough review of examples, experiments, and models where variability in mass transfer is documented or invoked.

Neretnieks and Rasmuson [1984] first applied the idea of diffusion within variable block sizes to the problem of radionuclide transport in fractured rocks. By introducing a "pseudobody", which models a distribution of block sizes with an approximate equivalent matrix body containing a distribution of layers, Neretnieks and Rasmuson were able to explore the importance of diffusion into nonuniform block sizes.

Ball and Roberts [1991a,b] performed a series of experiments examining sorptive uptake of organic compounds in the Borden sand. They found a strong correlation between grain radius and rates of uptake, suggesting that (1) intraparticle diffusion was responsible for rate-limited mass transfer and (2) multiple and simultaneous rates of mass transfer would be inherently important in natural porous media.

Pedit and Miller [1994, 1995] developed a stochastic model of mass transfer that allows nonlinear sorption and either spherical diffusion or first-order mass transfer. Using this formulation, they modeled mass transfer in a batch reactor using statistical distributions of rate coefficients. With distributions of rate coefficients they were able to significantly improve their representation of mass transfer relative to that offered by conventional models where rate coefficients are single-valued and deterministic. In addition, *Pedit and Miller* [1995] report estimated variations in effective diffusion rate coefficients of several orders of magnitude for a sediment containing a mixture of very fine to very coarse sand.

Grathwohl and Kleineidam [1995] measured sorptive uptake of phenanthrene into several different mineralogical and size fractions of the Horkheim aquifer. They modeled the bulk sample using a multicomponent version of *Crank's* [1975] spherical diffusion equation, which assumes a zero-concentration boundary on the spheres. Their results show that equilibrium is achieved in some fractions of the aquifer within a few days, while in other fractions of the aquifer, nonequilibrium conditions likely persist for many decades, indicating that effective diffusion rate coefficients may be spread over many orders of magnitude in natural materials.

Haggerty and Gorelick [1995] showed that linear models of mass transfer (e.g., first-order mass transfer, Fickian diffusion, diffusion into a distribution of regions in parallel or series, or combinations of first-order mass transfer and diffusion) can all be described mathematically by a mass transfer model with a distribution of first-order rate coefficients. For example, diffusion into a spherical immobile region is mathematically equivalent in every way (in terms of its effects on an advecting-dispersing plume) to first-order mass transfer into a distribution of immobile regions. Equivalently, a statistical distribution of immobile regions can be described using a first-order model with a different statistical distribution. *Haggerty and Gorelick* [1995] used this model to show that neither spherical diffusion or first-order mass transfer are adequate in many circumstances to predict long-term transport of solutes. They also used their model to predict mass transfer in a distribution of grain sizes of the Borden sand. *Haggerty and Gorelick* [1998]

showed that even in relatively homogeneous porous media, extreme variability (exceeding four orders of magnitude) in diffusion rate coefficients (D_d/a^2) must be invoked to explain solute transport in some media. Additionally, they demonstrated that neither a spherical diffusion model nor a model of first-order mass transfer with a single rate coefficient are capable of modeling mass transfer where such variability exists.

A conventional model of mass transfer assumes diffusive mass transfer can be described by a single effective diffusion coefficient and a single effective block size (typically either spherical or layered in shape). These effective parameters are typically combined into a diffusion rate coefficient (D_d/a^2). Such a model will be appropriate in cases where both of the following criteria are met: (1) the time-scale of the experiments from which D_d/a^2 is measured is approximately the same as the time-scale over which predictions of solute transport are needed; **and** (2) very accurate description of the tail of breakthrough curves are not needed. Two notable examples where one of these two criteria are violated are nuclear waste disposal (time-scale of measurement and prediction are different by a very large margin) and aquifer remediation (if predictions of time-to-cleanup are required, an accurate description of the breakthrough curve tail is needed).

The basic model of mass transfer envisioned and modeled within STAMMT-R is shown in Figure 1. In this model a statistical distribution of (D_d/a^2) is allowed. Solute is transported between immobile zones where water is stagnant. The properties of these immobile zones vary in the ways listed above, and in such a way as to provide a

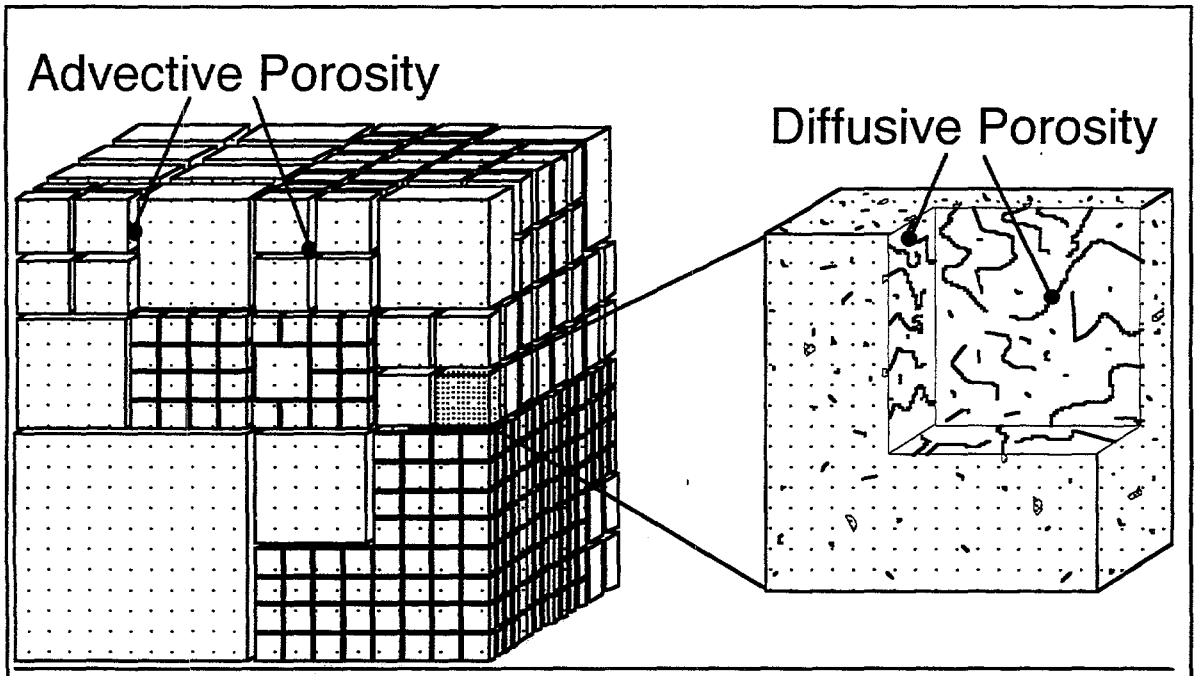

Figure 1: Schematic of mass transfer model invoked within STAMMT-L. Advective porosity lies between a mixture of matrix blocks of various sizes, each of which contains a range of different types of diffusive porosity.

continuous distribution of multirate diffusion rate coefficients for a layered system. By layered, we simply mean that the immobile zones in the model in Figure 1 are one-dimensional pathways contained within a three-dimensional matrix block - i.e., diffusion is mathematically equivalent to diffusion in a distribution of layers. Since the immobile zones are one-dimensional (although they may be tortuous), they may be each described by a diffusion equation with one Cartesian coordinate (i.e., layers).

2.2. Single-Well Injection-Withdrawal

The advective-dispersive-mass-transfer equations solved by this portion of the code are for conditions of radial flow to and from a single-well. The solution is performed in three steps: (1) injection; (2) rest; and (3) withdrawal. In each step, the Laplace-domain analytic solution is numerically inverted to the time-domain. Those concentrations are then used as initial conditions in the following step.

2.2.1. Radially Divergent Transport from an Injection Well

We first describe the model for radially divergent solute transport from an injection well, in the presence of a lognormal distribution of diffusion processes. Mass transfer is governed by diffusion into a distribution of one-dimensional pathways (see Figure 1). These pathways may be thought of as individual diffusion pathways within a matrix block, each with a different diffusion rate coefficient. If the user chooses a distribution with no variability (i.e., $\sigma = 0$), the model switches to a simulation of diffusion into spherical matrix blocks, each with the same diffusion rate coefficient (classic double-porosity model). The equations describing advective-dispersive transport in the presence of a lognormal distribution of rate-limited mass transfer processes are [after *Haggerty and Gorelick*, 1998]

$$\frac{\partial c}{\partial t} + \int_0^\infty b(\alpha_d) \frac{\partial \bar{s}(\alpha_d)}{\partial t} d\alpha_d = \frac{1}{r}\frac{\partial}{\partial r}\left(\frac{r\alpha_L v}{R_f}\frac{\partial c}{\partial r}\right) - \frac{v}{R_f}\frac{\partial c}{\partial r} \tag{1}$$

$$b(\alpha_d) = \frac{\beta_{tot}}{\sqrt{2\pi}\sigma\alpha_d} \exp\left\{-\frac{\left[\ln(\alpha_d) - \mu^*\right]^2}{2\sigma^2}\right\} \tag{2a}$$

where

$$\alpha_d \equiv \frac{D_a}{a^2} \tag{2b}$$

and

$$\beta_{tot} = \frac{\phi_m}{R_f \phi_f} \tag{2c}$$

and where c $[M\,L^{-3}]$ is the solute concentration in the fracture; $\bar{s}$ $[M\,L^{-3}]$ is the average solute concentration in a particular pathway in a matrix block; $b(\alpha_d)$ $[T^{-1}]$ is the lognormal probability density function (PDF) of diffusion rate coefficients; β_{tot} [-] is the total capacity coefficient of the formation; α_d $[1/T]$ is the diffusion rate coefficient; α_L $[L]$ is the longitudinal dispersivity; v $[L/T]$ is the pore-water velocity; R_f [-] a retardation factor,

representing retardation due to equilibrium sorption within the primary porosity (e.g., sorption to fracture walls); r [L] is the radial coordinate (positive away from well); t [T] is time; σ is the standard deviation of the log-transformed diffusion rate coefficients; μ^* is the log of the geometric mean of the diffusion rate coefficients; D_a [L^2/T] is the apparent diffusion coefficient; a [L] is the length of the diffusion pathway within the matrix; ϕ_m [-] is the matrix porosity of the formation; and ϕ_f [-] is the fracture porosity.

Equation (1) is similar to conventional equations of solute transport with mass transfer, with the modification to account for a distribution of mass transfer domains. Instead of having movement of mass either into or out of a single immobile domain, equation (1) allows for simultaneous movement into and out of a continuous distribution of immobile zones with different characteristics. The mass transfer into and out of all immobile domains is summed using the integral term in (1).

STAMMT-R assumes a lognormal distribution of layered diffusion rate coefficients D_a/a^2 to describe the variability of diffusion within the matrix. Variation in D_a/a^2 can be ascribed to several different sources including diffusion path length, sorption strength (if present), and the diameter of the micropore in the direction perpendicular to diffusion [*Satterfield et al.*, 1973]. Since natural materials contain mixtures of minerals and pore structures, typical distributions of diffusion rate coefficients should be viewed as lumped expressions of processes occurring in series and in parallel. The lognormal distribution is the only statistical distribution currently available within STAMMT-R. The lognormal distribution is selected primarily due to its ease of use: however, there is some independent evidence to suggest a lognormal distribution is a good choice. Several geological properties frequently appear to be lognormally or nearly lognormally distributed, including hydraulic conductivity [*Neuman*, 1982; *Hoeksema and Kitanidis*, 1985] and grain size [*Buchan*, 1989; *Buchan et al.*, 1993]. It also may be that the distribution coefficient and the sizes (both length and diameter) of micropores are approximately lognormally distributed. The products or quotients of independent random variates from a lognormal distribution produce another lognormal distribution [*Aitchison and Brown*, 1957, p. 11]. Additionally, the product of many independent, positive variates is also lognormally distributed [*Aitchison and Brown*, 1957, p. 14]. Therefore, since properties of a medium such as grain size and the distribution coefficient contribute multiplicatively to the diffusion rate coefficient D_a/a^2 [*Haggerty and Gorelick*, 1998], we hypothesize that the diffusion rate coefficient itself may be lognormally distributed.

A typical lognormal distribution used in STAMMT-R is shown in Figure 2. This lognormal distribution has $\mu^* = -8$ (where D_a/a^2 has units of hr^{-1}) and $\sigma = 3.0$. As such, the diffusion rate coefficient varies over several orders of magnitude. As a corollary, the time-scales of mass transfer would also vary over several orders of magnitude. A number of other distributions (shown as CDFs rather than PDFs) of rate coefficients may be seen in *Werth et al.* [1997] and *Haggerty and Gorelick* [1998].

It is assumed within STAMMT-R that the tracer may sorb within the advective porosity, but not within the matrix porosity. However, it is a simple matter to invoke linear sorption within the matrix: set the matrix porosity (ϕ_m) to the value of $\phi_m R_m$, where R_m is the retardation factor due to sorption within the matrix and is greater than

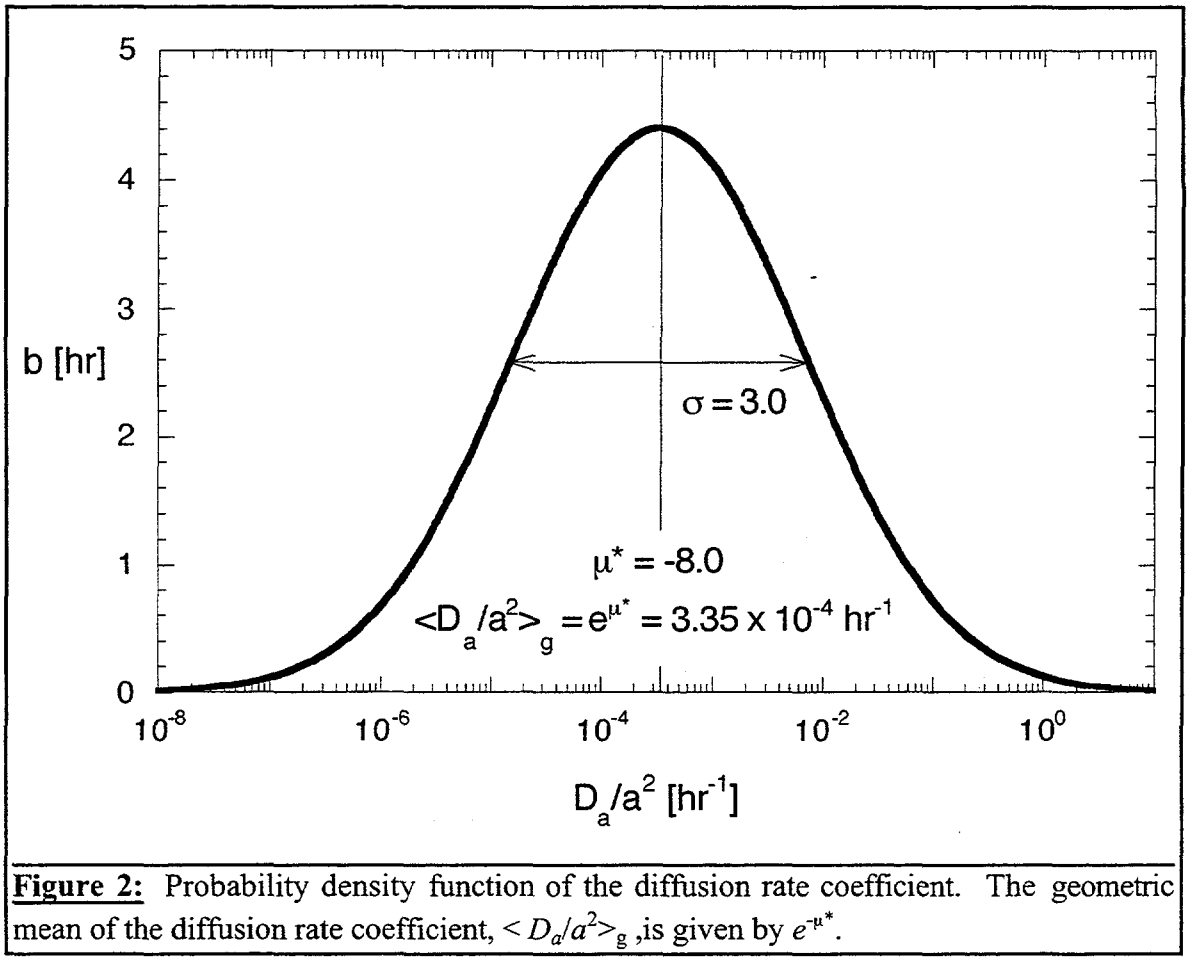

Figure 2: Probability density function of the diffusion rate coefficient. The geometric mean of the diffusion rate coefficient, $< D_a/a^2 >_g$,is given by e^{μ^*}.

unity only if there is sorption. Sorption is assumed linear and may be invoked within the fracture by setting R_f greater than 1.

All parameters in equations (1) and (2) are homogeneous in space. The variability in the mass transfer rate coefficients is assumed to exist at a point. In other words, it is assumed that the model scale is significantly larger than the correlation scale for variability within the mass transfer processes. This assumption is justified in many cases because heterogeneity in diffusive processes is often at a very small scale of mm to cm [e.g., *Christian-Frear et al.*, 1997; *Werth et al.*, 1997; *Xu and Worman*, 1997; *Haggerty and Gorelick*, 1998].

The time-derivative of the average solute concentration in a particular pathway within the matrix is given by:

$$\frac{\partial\, \bar{s}(\alpha_d)}{\partial t} = \frac{1}{a}\int_0^a \frac{\partial\, s(\alpha_d)}{\partial t}\, dz \;, \qquad 0 < \alpha_d < \infty \tag{3a}$$

where s $[M/L^3]$ is the concentration at a point within the matrix; and z $[L]$ is the coordinate along the pathway. The concentration within a given diffusion pathway in the matrix is given by the solution to the diffusion equation:

$$\frac{\partial s(\alpha_d)}{\partial t} = D_a \frac{\partial^2 s(\alpha_d)}{\partial z^2}, \quad 0 < \alpha_d < \infty \tag{3b}$$

Problem Solution:

To solve this problem for the injection phase, we use the multirate approach outlined in Section 2.3, where we replace (1), (2a), (3a), and (3b) with the following three equations, derived in Section 2.4 (also see *Haggerty and Gorelick* [1998] for a very similar treatment in linear coordinates and dimensionless form):

$$\frac{\partial c}{\partial t} + \int_0^\infty b(\alpha_m) \frac{\partial s_m(\alpha_m)}{\partial t} d\alpha_m = \frac{1}{r} \frac{\partial}{\partial r} \left(\frac{r \alpha_L v}{R_f} \frac{\partial c}{\partial r} \right) - \frac{v}{R_f} \frac{\partial c}{\partial r} \tag{4a}$$

$$\frac{\partial s_m(\alpha_m)}{\partial t} = \alpha_m \left[c - s_m(\alpha_m) \right], \quad 0 < \alpha_m < \infty \tag{4b}$$

$$b(\alpha_m) = \sum_{j=1}^{\infty} \frac{8 \beta_{tot}}{\sqrt{2\pi^5} (2j-1)^2 \sigma \alpha_m} \exp \left\{ - \frac{\left[\ln \left(\frac{4 \alpha_m}{\pi^2 (2j-1)^2} \right) - \mu^* \right]^2}{2\sigma^2} \right\} \tag{5}$$

where $s_m(\alpha_m)$ $[M/L^3]$ are the concentrations in a continuous distribution of immobile zones with differing first-order rate coefficients, α_m. All other parameters given above are the same as before. For a discussion of the mathematical steps taken above, see Section 2.4. Equation (5) shows the replacement of the lognormal distribution in (2a) with a distribution of first-order rate coefficients that is equivalent to it [*Haggerty*, 1995; *Haggerty and Gorelick*, 1998]. Note also that since (4a) and (4b) have as their basis the first-order model of mass transfer, that these equations can also be used in the code to model solute transport with either a non-parametric distribution of first-order mass transfer rate coefficients (including conventional first-order mass transfer) or spherical diffusion. See Section 2.4 for a discussion of the distribution needed to make (4a) and (4b) equivalent to spherical diffusion.

The pore-water velocity in (1) and (4a) is given by:

$$v = \frac{Q}{2\pi r \phi_f b_f} \tag{6}$$

where Q $[L^3/T]$ is the pumping rate or injection rate; ϕ_f [-] is the fracture porosity; and b_f $[L]$ is the formation thickness. The boundary conditions for (1) and (4a) are:

$$c - \alpha_L \frac{\partial c}{\partial r} = c_{inj} \qquad at\ r = r_w \tag{7a}$$

$$\frac{\partial c}{\partial r} = 0 \qquad r \to \infty \tag{7b}$$

where r_w [L] is the well radius and c_{inj} [M/L^3] is the injected concentration. Equation (7a) is the standard Couchy (third type) boundary condition [e.g., *Kreft and Zuber*, 1978; *de Marsily*, 1986] accounting for both advective and dispersive flux across the inlet boundary. Initial conditions are that concentrations (both matrix and fracture) are initially zero.

This problem can be nondimensionalized with the following:

$$T = \frac{Qt}{2\pi b_f \phi_f \alpha_L^2 R_f} \tag{8a}$$

$$\omega_m = \alpha_m \frac{2\pi b_f \phi_f \alpha_L^2 R_f}{Q} \tag{8b}$$

$$\rho = \frac{r}{\alpha_L} \tag{8c}$$

$$\rho_\omega = \frac{r_w}{\alpha_L} \tag{8d}$$

For our purposes, we do not bother nondimensionalizing concentration as its nondimensional form does not change the solution. Using these nondimensional forms, as well as the changes to the multirate formulation, we arrive at the following equations for solute transport and mass transfer:

$$\frac{\partial c}{\partial T} + \int_0^\infty b(\omega_m) \frac{\partial s_m(\omega_m)}{\partial T} d\alpha_m = \frac{1}{\rho}\left(\frac{\partial^2 c}{\partial \rho^2} - \frac{\partial c}{\partial \rho}\right) \tag{9}$$

$$\frac{\partial s_m}{\partial T} = \omega_m (c - s_m) \tag{10}$$

$$b(\omega_m) = \sum_{j=1}^{\infty} \frac{8\beta_{tot}}{\sqrt{2\pi^5}(2j-1)^2 \sigma \omega_m} \exp\left\{ - \frac{\left[\ln\left(\frac{4\omega_m}{\pi^2(2j-1)^2}\right) - \mu\right]^2}{2\sigma^2} \right\} \tag{11}$$

where μ [-] is the log of the geometric mean of the nondimensional rate coefficients and σ is as previously defined. The relationship between the dimensional and dimensionless forms of μ are given by:

$$\mu^* = \mu + \ln\left(\frac{Q}{2\pi b_f \phi_f \alpha_L^2}\right) \tag{12}$$

The boundary conditions become:

$$c - \frac{\partial c}{\partial \rho} = c_{inj} \qquad at\ \rho = \rho_w \tag{13a}$$

$$\frac{\partial c}{\partial \rho} = 0 \qquad \rho \to \infty \tag{13b}$$

The Laplace transform of (9) and (10) are, respectively,

$$p\,\bar{c} + p\int_0^\infty b(\omega_m)\,\overline{s_m(\omega_m)}\,d\alpha_m = \frac{1}{\rho}\left(\frac{\partial^2 \bar{c}}{\partial \rho^2} - \frac{\partial \bar{c}}{\partial \rho}\right) \tag{14}$$

$$p\,\overline{s_m} = \omega_m\left(\bar{c} - \overline{s_m}\right) \tag{15}$$

which can be rearranged to:

$$\overline{s_m} = \frac{\omega_m \bar{c}}{p + \omega_m} \tag{16}$$

where p is the Laplace parameter and an overbar indicates the Laplace transform of a variable. Substituting (16) into (14) and rearranging yields:

$$\frac{\partial^2 \bar{c}}{\partial \rho^2} - \frac{\partial \bar{c}}{\partial \rho} - \rho\, p\left[1 + \int_0^\infty \frac{b(\omega_m)\,\omega_m}{p + \omega_m}\,d\omega_m\right]\bar{c} = 0 \tag{17}$$

The boundary conditions become:

$$\bar{c} - \frac{\partial \bar{c}}{\partial \rho} = \overline{c_{inj}} \qquad at\ \rho = \rho_w \tag{18a}$$

$$\frac{\partial \bar{c}}{\partial \rho} = 0 \qquad \rho \to \infty \tag{18b}$$

Note that the injected concentrations must be transformed into the Laplace domain. Although it is a simple matter to use a non-uniform injected concentration, we will assume that injected concentrations begin at zero, then go instantaneously to a uniform value for a given pulse length, and then instantaneously return to zero. A future version of the code may be modified to handle time-varying input concentrations. The Laplace transform of this "square wave" is:

$$\overline{c_{inj}} = c_{inj}\frac{\exp\left(p\,T_0\right) - \exp\left(p\,T_E\right)}{p} \tag{19}$$

where T_0 [-] is the beginning dimensionless time for the pulse, and T_E [-] is the ending dimensionless time for the pulse.

Chen [1985] shows that an equation very similar to (17) can be transformed to the homogeneous Airy equation (see Appendix A of *Chen* [1985]). We define the following variable to simplify the resulting expressions:

$$\mathcal{P} = p\left[1 + \int_0^\infty \frac{b(\omega_m)\,\omega_m}{p + \omega_m}\, d\omega_m\right] \tag{20}$$

Using this variable, we can re-write (17) as:

$$\frac{\partial^2 \hat{c}}{\partial \rho^2} - \frac{\partial \hat{c}}{\partial \rho} - \rho\,\mathcal{P}\,\hat{c} = 0 \tag{21}$$

The general solution to this equation [*Chen*, 1985] is:

$$\hat{c} = A_1 \exp\left(\frac{y}{2}\right) \mathrm{Ai}\left(\mathcal{P}^{1/3} y\right) + A_2 \exp\left(\frac{y}{2}\right) \mathrm{Bi}\left(\mathcal{P}^{1/3} y\right) \tag{22}$$

where A_1 and A_2 are functions yet to be determined; Ai(*) and Bi(*) are Airy functions; and

$$y = \rho + \frac{1}{4\mathcal{P}} \tag{23}$$

Solving with our boundary conditions (not shown here), we arrive at the following solution to (14):

$$\hat{c} = \overline{c_{inj}} \exp\left(\frac{\rho - \rho_0}{2}\right) \frac{\mathrm{Ai}\left(\mathcal{P}^{1/3} y\right)}{\frac{1}{2}\mathrm{Ai}\left(\mathcal{P}^{1/3} y_0\right) - \mathcal{P}^{1/3}\mathrm{Ai}'\left(\mathcal{P}^{1/3} y_0\right)} \tag{24}$$

where Ai'(*) is the derivative of the Airy function and where y_0 indicates the value of y at $\rho = \rho_0$.

Equations (16) and (24) can be inverted to the time domain using a numerical Laplace inversion algorithm. For our purposes, we employed the *de Hoog et al.* [1982] algorithm as applied by the commercially available International Mathematics and Statistics Libraries (IMSL) Version 3.0 (see Section 3 for details on the availability of IMSL.). This algorithm is based on accelerating the convergence of the Fourier series obtained from the inversion integral using the trapezoidal rule [*de Hoog et al.*, 1982].

2.2.2. Resting Phase

During the resting phase of the push-pull test, it is assumed that advective velocities are zero. Therefore, (1) becomes:

$$\frac{\partial c}{\partial t} + \int_0^\infty b(\alpha_d) \frac{\partial\, \bar{s}(\alpha_d)}{\partial t}\, d\alpha_d = 0 \tag{25}$$

and (2a) through (3b) remain the same. To solve this problem, we also use the multirate formulation, replacing the integral in (25) with the integral in (4a) and replacing (2a), (3a), and (3b) with (4b) and (5). The initial conditions are that all concentrations are the same as those at the end of the injection period. The concentrations in the mobile zone (c) and immobile zones (s_m) are generally not at equilibrium at this time.

Equation (25) and those coupled to it can be solved by using the Laplace transform and inverse Laplace transform (or by other means as well, such as the matrix exponential [*Haggerty and Gorelick*, 1995]). In the Laplace domain, *after* converting to the multirate formulation, the solutions to the multirate equivalents of (25) and (3a) are as follows:

$$\bar{c} = \frac{c_0 + \int_0^\infty \frac{b(\alpha_m)\,\alpha_m}{p+\alpha_m} s_0(\alpha_m)\,d\alpha_m}{p\left[1 + \int_0^\infty \frac{b(\alpha_m)\,\alpha_m}{p+\alpha_m}\,d\alpha_m\right]} \tag{26}$$

and

$$\overline{s(\alpha_m)} = \frac{\alpha_m}{p+\alpha_m}\bar{c} + \frac{s_0(\alpha_m)}{p+\alpha_m} \tag{27}$$

where $s_o(\alpha_d)$ $[M/L^3]$ are the concentrations in the multirate immobile zones at the end of the injection phase.

Equations (26) and (27) can be inverted to the time domain using a numerical Laplace inversion algorithm. For our purposes, we employed the *de Hoog et al.* [1982] algorithm as applied by the commercially available International Mathematics and Statistics Libraries (IMSL) Version 3.0 (see Section 3 for details on the availability of IMSL.).

2.2.3. Withdrawal of Tracer from Pumping Well

Employing all nondimensional parameters used before, equations (6), and (8a) to (8d), we can again nondimensionalize (1) for radially convergent flow. In this case, the pumping rate is negative in (6). Using the same distributed mass transfer equations (2a), (3a) and (3b), and the multirate approach from Section 2.4. to solving them, we arrive at the following nondimensional equations:

$$\frac{\partial c}{\partial T} + \int_0^\infty b(\omega_m)\frac{\partial s_m(\omega_m)}{\partial T}\,d\alpha_m = \frac{1}{\rho}\left(\frac{\partial^2 c}{\partial \rho^2} + \frac{\partial c}{\partial \rho}\right) \tag{28}$$

$$\frac{\partial s_m}{\partial T} = \omega_m(c - s_m) \tag{29}$$

where (29) is the same as (10) but is rewritten here for the sake of completeness.

The boundary conditions employed are different from the divergent flow case:

$$\frac{\partial c}{\partial \rho} = 0 \qquad \rho = \rho_w \tag{30a}$$

$$c = 0 \qquad \rho \to \infty \tag{30b}$$

The initial conditions for both the mobile and immobile zones are taken as the concentrations at the end of the resting period.

The Laplace transform of (28) and (29), with non-zero initial conditions, are:

$$p\,\bar{c} - c_0 + \int_0^\infty b(\omega_m)\left[p\,\overline{s_m(\omega_m)} - s_{m,0}(\omega_m)\right] d\omega_m = \frac{1}{\rho}\left(\frac{\partial^2 \bar{c}}{\partial \rho^2} + \frac{\partial \bar{c}}{\partial \rho}\right) \tag{31}$$

and

$$\overline{s(\omega_m)} = \frac{\omega_m}{p + \omega_m}\bar{c} + \frac{s_0(\omega_m)}{p + \omega_m} \tag{32}$$

$$\frac{\partial^2 \bar{c}}{\partial \rho^2} + \frac{\partial \bar{c}}{\partial \rho} - \rho\, p\left[1 + \int_0^\infty \frac{b(\omega_m)\,\omega_m}{p + \omega_m} d\omega_m\right]\bar{c} + \rho\left[c_0 + \int_0^\infty \frac{b(\omega_m)\,\omega_m}{p + \omega_m} s_0(\omega_m)\, d\omega_m\right] = 0 \tag{33}$$

We also make the following definition:

$$\mathcal{F}(\rho) = c_0(\rho) + \int_0^\infty \frac{b(\omega_m)\,\omega_m}{p + \omega_m} s_0(\omega_m, \rho)\, d\omega_m \tag{34}$$

Note that $s_0(\omega_m, \rho)$ indicates that s_0 is a function of ω_m and ρ. In other locations, s_0 is also a function of ρ, but this was not emphasized as was done here. We can re-write (33) as:

$$\frac{\partial^2 \bar{c}}{\partial \rho^2} + \frac{\partial \bar{c}}{\partial \rho} - \rho\, \mathcal{P}\, \bar{c} = -\rho\, \mathcal{F}(\rho) \tag{35}$$

which can be re-arranged to form the inhomogeneous Airy equation. *Chen and Woodside* [1988] solved (35), with boundary conditions and initial conditions as we have expressed. Modifying their solution to solve only at $\rho = \rho_w$, we get the following:

$$\bar{c} = \exp\left(-\frac{\rho_0}{2}\right) \int_{\rho_0}^\infty \xi \exp\left(\frac{\xi}{2}\right) \mathcal{F}(\xi)\, g_1(\rho, s, \xi)\, d\xi \tag{36}$$

where $\mathcal{F}(\xi)$ is given in (34), y_0 is given in (23), and where:

$$g_1 = \frac{\pi}{\mathcal{P}^{1/3}} \mathrm{Ai}\left(\mathcal{P}^{1/3}\Lambda\right)\left[\mathrm{Bi}\left(\mathcal{P}^{1/3} y_0\right) - X\,\mathrm{Ai}\left(\mathcal{P}^{1/3} y_0\right)\right] \tag{37}$$

$$X = \frac{\wp^{1/3}\,\mathrm{Bi}'\left(\wp^{1/3}y_0\right) - \frac{1}{2}\,\mathrm{Bi}\left(\wp^{1/3}y_0\right)}{\wp^{1/3}\,\mathrm{Ai}'\left(\wp^{1/3}y_0\right) - \frac{1}{2}\,\mathrm{Ai}\left(\wp^{1/3}y_0\right)} \tag{38}$$

$$\Lambda = \xi + \frac{1}{4\wp} \tag{39}$$

Equation (36) can be inverted to the time domain using a numerical Laplace inversion algorithm. Again, we employ the *de Hoog et al.* [1982] algorithm as applied by the commercially available International Mathematics and Statistics Libraries (IMSL) Version 3.0 (see Section 3 for IMSL availability). We find that the inverse solution for convergent flow takes significantly longer than the inverse solutions for divergent flow and the resting phase (typically the latter takes a few seconds, whereas the convergent flow solution may take many minutes on a Silicon Graphics Indigo 2 with an R10000 chip and 128 MB RAM). This is primarily because of the integral in (36) that must be evaluated numerically many thousands or tens of thousands of times during an inverse solution.

2.3. Two-well Injection-Withdrawal

2.3.1. Injection of Tracer at First Well

Injection of a tracer at the first well of a two-well injection-withdrawal problem is handled by the same analytic solution as injection for a single-well injection-withdrawal problem, discussed in Section 2.2.1. We assume that extraction of water at the pumping well does not significantly affect the flow field near the injection well. Using this assumption, the shape of the injected tracer would be a perfect ring; however, if the assumption is violated, the tracer would take on an oblong shape. In general, the assumption will be valid provided that (1) the ratio of the volume of tracer and chaser to the formation volume in the vicinity of the two wells is small; and (2) the ratio of the velocity near the injection well due to injection divided by the velocity at the same location due to pumping is large. Mathematically these can be expressed, respectively, as (after *Guvanasen and Guvanasen*, 1987):

$$\frac{Q_{in}\left(t_{in} - t_0\right)}{\pi b \phi_f R_0} << 1 \tag{40}$$

$$\frac{Q_{in} R_0}{Q_{out} r_w} >> 1 \tag{41}$$

where Q_{in} $[L^3/T]$ is the injection rate of the tracer and chaser; t_{in} $[T]$ is the elapsed time to the end of tracer and chaser injection; t_0 $[T]$ is the elapsed time before tracer and chaser injection start; R_0 $[L]$ is the distance from the pumping to the injection well; Q_{out} $[L^3/T]$ is the pumping rate; and r_w $[L]$ is the radius of the injection well. For a detailed discussion of the shapes of injected tracers during pumping from a second well, the reader is referred to *Guvanasen and Guvanasen* [1987].

2.3.2. Withdrawal of Tracer from Pumping Well

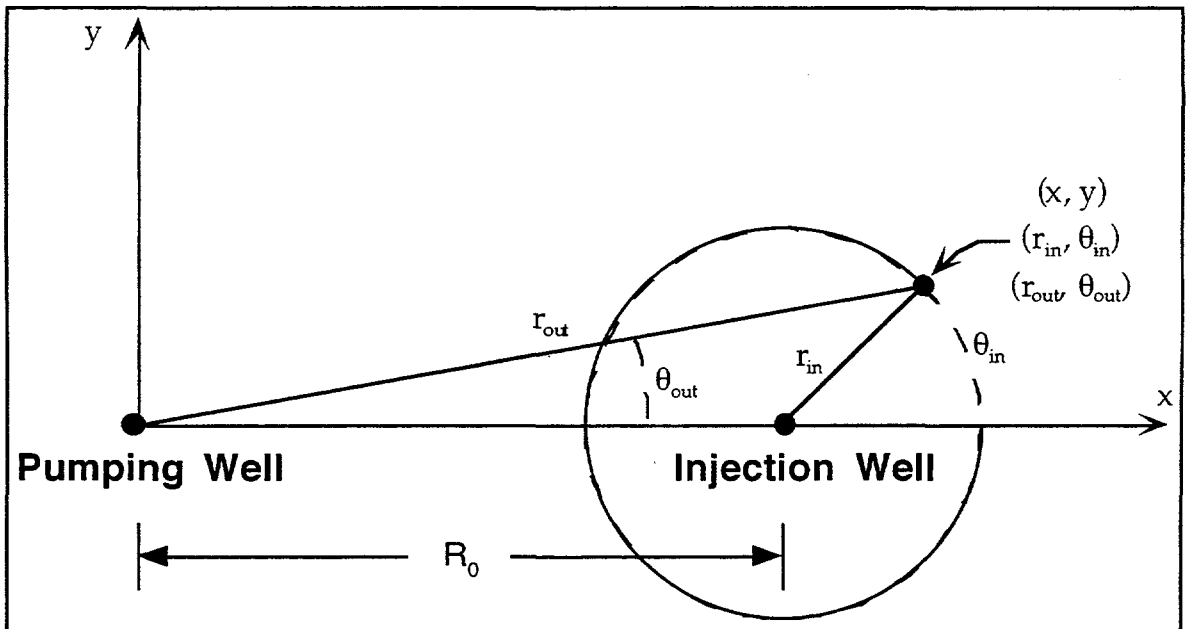

Figure 3: Schematic of polar coordinate transformation from coordinates with respect to the injection well to coordinates with respect to the pumping well.

Once we inject solute at the injection well, we must then calculate the breakthrough curve at the pumping well. We perform this calculation in three steps: (1) transform polar coordinates relative to the injection well (r_{in}, θ_{in}) to coordinates relative to the pumping well (r_{out}, θ_{out}); (2) azimuthally average the concentrations; (3) calculate the breakthrough curve at the pumping well for azimuthally averaged concentrations. These three steps, which are described in detail below, allow us to find a semi-analytical solution for the breakthrough curve at the pumping well. In fact, this semi-analytical solution turns out to be the same as that given for convergent flow in Section 2.2.3, and therefore allows us to take advantage of much of the code already written for the single-well injection-withdrawal problem.

Coordinate Transformation:

First, we transform the polar coordinates from the injection well to the pumping well. Figure 3 shows the relationship between the polar coordinate system with respect to the two wells, in addition to an "intermediate" Cartesian coordinate system that may be used to derive the transformation (i.e., $x = r_{out} \cos \theta_{out} = R_0 + r_{in} \cos \theta_{in}$ and $y = r_{out} \sin \theta_{out} = r_{in} \sin \theta_{in}$). Based on the law of cosines, the transformations from the injection well coordinate system to the pumping well coordinate system are given:

$$r_{out} = \sqrt{R_0^2 + 2R_0 r_{in} \cos \theta_{in} + r_{in}^2} \tag{42a}$$

$$\theta_{out} = \tan^{-1}\left(\frac{r_{in} \sin \theta_{in}}{R_0 + r_{in} \cos \theta_{in}}\right) \tag{42b}$$

Azimuthal Averaging:

The next step after coordinate transformation is to reduce the dimensionality of the problem from two to one (in addition to time and the coordinate system for mass transfer). Solute transport toward the pumping well as shown in Figure 3 would require solution of a system of integro-differential equations in r_{out}, θ_{out}, and t. However, by using azimuthal averaging, we can eliminate θ_{out} [*Zlotnik and Logan*, 1996] in our problem.

Azimuthal averaging takes all concentrations at a distance r from the pumping well and averages them. In a formation that is homogeneous with respect to thickness, fracture porosity, and hydraulic conductivity, all mass at a given distance from the pumping well will experience the same velocity and similar dispersion as it moves toward the well. Therefore, concentrations can be averaged and then transport simulated in one dimension rather than two.

The azimuthally averaged concentration at the beginning of convergent simulation (end of injection, t_0) is defined by [*Zlotnik and Logan*, 1996]:

$$c\left(r_{out}, t_0\right) = \frac{1}{2\pi}\int_{-\pi}^{\pi} c\left(r_{out}, \theta_{out}, t_0\right) d\theta_{out} \tag{43}$$

In practice, this integral need not be evaluated over the entire range $[-\pi, \pi]$, but only over the interval where there is non-zero concentration.

Calculation of Breakthrough Curve for Convergent Flow:

Once the azimuthal averaging of concentrations has been performed, calculation of the breakthrough curve at the well is precisely the same as the solution and calculation discussed in Section 2.2.3. The reader is referred to that section and the solution is not reproduced here.

2.4. Theory of Multirate Mass Transfer

In this section we show the extended multirate approach of *Haggerty* [1995] and *Haggerty and Gorelick* [1995] for a continuous lognormal distribution of immobile zones. Much of this was published by *Haggerty and Gorelick* [1998]. A related discussion can be found in *Carrera et al.* [1998].

Haggerty and Gorelick [1995] show that a series of first-order mass transfer equations with a specific distribution of rate and capacity coefficients is precisely and mathematically equivalent to diffusion. First, we substitute a new integral of concentration derivatives into (1):

$$\int_0^\infty b\left(\alpha_d\right)\frac{\partial\, \overline{s}\left(\alpha_d\right)}{\partial t} d\alpha_d = \int_0^\infty b\left(\alpha_m\right)\frac{\partial\, s_m\left(\alpha_m\right)}{\partial t} d\alpha_m \tag{44a}$$

This substitution is shown in (4a). The derivatives in (44a) are continuously distributed in α_d and α_m over $(0, \infty)$. This continuously distributed derivative is equated with a first-order mass transfer relationship that replaces equations (3a) and (3b):

$$\frac{\partial s_m(\alpha_m)}{\partial t} = \alpha_m \left[c - s_m(\alpha_m) \right], \qquad 0 < \alpha_m < \infty \tag{44b}$$

where α_m [$1/T$] are the rate coefficients of the immobile zones; $b(\alpha_m)$ is the probability density function (PDF) describing the distribution of rate coefficients; and s_m [M/L^3]. are the concentrations in those immobile zones.

Expressions given by *Haggerty and Gorelick* [1995, p. 2389] employ a discrete form of the right hand sides of (44a) and (44b) and show that, for specific forms of α_m and $b(\alpha_m)$, these are mathematically precisely equivalent to solute transport with diffusion into and out of spheres, cylinders, or layers. The discrete forms of (44a) and (44b) are:

$$\int_0^\infty b(\alpha_d) \frac{\partial \bar{s}(\alpha_d)}{\partial t} d\alpha_d = \sum_{j=1}^{\infty} \beta_j \frac{\partial s_{m,j}}{\partial t} \tag{45a}$$

$$\frac{\partial s_{m,j}}{\partial t} = \alpha_{m,j} \left[c - s_{m,j} \right], \qquad j = 1, 2, \cdots \infty \tag{45b}$$

The following two series, called the "multirate series", make (45a) and (45b) equivalent to diffusion into or out of a single one-dimensional pathway:

$$\alpha_{m,j} = \frac{(2j - 1)^2 \pi^2 \alpha_d}{4}, \qquad j = 1, 2, \cdots \infty \tag{46a}$$

$$\beta_j = \frac{8\beta_{tot}}{(2j - 1)^2 \pi^2}, \qquad j = 1, 2, \cdots \infty \tag{46b}$$

where β_{tot} is the total capacity coefficient given in (2c). *Carrera et al.* [1998] showed equations (46a) and (46b) to be correct using a derivation from an integro-differential equation describing solute transport. Use of (46a) and (46b) in practice requires truncation of the series. This truncation is discussed in Section 2.4.1 for the case of spheres, with mention of the layered (1-D pathway) case at the end of the Section.

To use the multirate approach for the distributed diffusion model, we must find the continuous multirate distribution that is equivalent to a lognormal distribution of diffusion rate coefficients. In other words, we wish to convert $b(\alpha_d)$ in (1) and (2a) to $b(\alpha_m)$. We do this using the intermediate discrete form of $b(\alpha_{m,j})$. The relationship between $b(\alpha_d)$ and $b(\alpha_{m,j})$ is given by (e.g., *Thomas*, 1986, p. 159):

$$\beta(\alpha_{m,j}) = \beta\left(g(\alpha_{m,j})\right) \left| \frac{d\left(g(\alpha_{m,j})\right)}{d\alpha_{m,j}} \right| \tag{47}$$

where $g(\alpha_{m,j})$ is the inverse of the function given in (46a), i.e.,

$$\alpha_d = g\left(\alpha_{m,j}\right) = \frac{4\,\alpha_{m,j}}{\left(2j-1\right)^2\pi^2}, \qquad j = 1, 2, \cdots \infty \tag{48}$$

The conversion of the PDF in (2a) from α_d to α_m must be done for each j of the discrete form and then summed over all values. After inserting (2a) and (48) into (47), we get

$$b\left(\alpha_{m,j}\right) = \frac{\beta_{tot}}{\sqrt{2\pi}\,\sigma\alpha_{m,j}} \exp\left\{ - \frac{\left[\ln\left(\frac{4\,\alpha_{m,j}}{\pi^2\left(2j\text{-}1\right)^2} \right) - \mu^* \right]^2}{2\sigma^2} \right\}, \qquad j = 1, 2, \cdots \infty \tag{49}$$

Equation (49) represents an infinite number of distributions. Since each of them are continuous on $\alpha_{m,j}$ we can sum them together in the proportions given in (46b), which represents the weight of each distribution j. Performing this summation and re-arranging, we get:

$$b\left(\alpha_m\right) = \sum_{j=1}^{\infty} \frac{8\,\beta_{tot}}{\sqrt{2\pi^5}\left(2j\text{-}1\right)^2\sigma\alpha_m} \exp\left\{ - \frac{\left[\ln\left(\frac{4\,\alpha_m}{\pi^2\left(2j\text{-}1\right)^2} \right) - \mu^* \right]^2}{2\sigma^2} \right\} \tag{50}$$

Note that the subscript j is no longer necessary on α_m because all values of α_m are now continuous over the same range, $(0, \infty)$. Equation (50) is equal to equation (5).

The PDF in (50) is the multirate equivalent of the distributed diffusion model with a lognormal distribution of α_d. Mass transfer with either model is completely equivalent in every respect. To use the multirate distribution in (50), we can either substitute it directly into (44a) and then (1), or substitute a discrete form of (50) in (45a) and then (1). We chose the latter and discretized $b(\alpha_m)$ such that both the PDF and associated CDF are exact at each discretization node. Mathematically, this is done as:

$$\beta_j = \int_{\alpha_{j-1/2}}^{\alpha_{j+1/2}} b\left(\alpha_m\right) d\alpha_m, \qquad 0 \le \alpha_m < \infty \tag{51}$$

2.4.1. Discussion of Multirate Mass Transfer and Spherical Diffusion

It is possible to use the multirate model of mass transfer to simulate spherical diffusion [*Haggerty and Gorelick*, 1995]. The multirate series that make (45a) and (45b) equivalent to diffusion into or out of a spheres are the following:

$$\alpha_{m,j} = j^2\pi^2\alpha_d, \qquad j = 1, 2, \cdots \infty \tag{52a}$$

$$\beta_j = \frac{6\beta_{tot}}{j^2\pi^2}, \qquad j = 1, 2, \cdots \infty \tag{52b}$$

where β_{tot} is the total capacity coefficient given in (2c).

In using (52a) and (52b) it is clear that we are not able to use the entire infinite series. In STAMMT-R, the series is truncated (under the current, QA'd version of the code) at 35. To maximize the accuracy of STAMMT-R, the truncated series is calculated precisely as (52a) and (52b) indicate up to the N^{th} rate coefficient (where N = **nm** and is 35 in the current version of the code). The N^{th} capacity coefficient (β_N) is given the weight of the remainder of the infinite series, and the N^{th} rate coefficient is calculated in such a way that the harmonic means of the truncated and the infinite series are identical. This ensures that the 0th, 1st, and 2nd temporal moments of breakthrough curves are identical to those that would result from the infinite series (see *Harvey and Gorelick*, 1995 for a discussion of temporal moments in the context of mass transfer). The harmonic mean of the infinite series for the case of spherical diffusion is given by $15\alpha_d$ [*Haggerty and Gorelick*, 1995]. Therefore, for the truncated series we require that the following hold true:

$$\left[\sum_{j=1}^{N-1}\frac{\beta_j}{\beta_{tot}\alpha_{m,j}} + \sum_{j=N}^{\infty}\frac{\beta_j}{\beta_{tot}\alpha_{m,N}}\right]^{-1} = 15\alpha_d \tag{53}$$

Solving for $\alpha_{m,N}$ we get:

$$\alpha_{m,N} = \frac{\sum_{j=N}^{\infty}\beta_j}{\frac{\beta_{tot}}{15\alpha_d} - \sum_{j=1}^{N-1}\frac{\beta_j}{\alpha_{m,j}}} \tag{54}$$

We can substitute (52a) and (52b) into (54) and arrive at:

$$\alpha_{m,N} = \frac{\alpha_d\sum_{j=N}^{\infty}\frac{1}{j^2\pi^2}}{\frac{1}{90} - \sum_{j=1}^{N-1}\frac{1}{j^4\pi^4}} = \frac{\alpha_d\left[\frac{1}{6} - \sum_{j=1}^{N-1}\frac{1}{j^2\pi^2}\right]}{\frac{1}{90} - \sum_{j=1}^{N-1}\frac{1}{j^4\pi^4}} \tag{55}$$

In the case of spherical diffusion and N=35, then equation (55) can be simplified to:

$$\alpha_{m,N} \simeq 35254\ \alpha_d \tag{56}$$

If the time-scale of transport (first breakthrough) is earlier than approximately $(\alpha_{m,N})^{-1}$ and the model is being run with $\sigma = 0$ (spherical diffusion), then the user is advised that

the earliest portions of the resulting breakthrough curve may be inaccurate. This will particularly be true if the β_{tot} is greater than 50.

For example let us look at a problem where β_{tot} is 200 and the desired model is spherical diffusion. If the half-block size is 1.0 m, the diffusivity is 7.3 x 10^{-10} m^2/s, the tortuosity is 0.11, then α_d is 8.03 x 10^{-11} /s. Consequently, if the first breakthrough time is earlier than approximately 3.5 x 10^5 s (97.2 hr), the early-time breakthrough curve will contain some inaccuracies.

An very similar derivation can be made for the case of layers or 1-D pathways. In this case, (55) becomes

$$\alpha_{m,N} = \frac{\alpha_d \sum_{j=N}^{\infty} \frac{1}{(2j-1)^2\pi^2}}{\frac{1}{24} - \sum_{j=1}^{N-1} \frac{4}{(2j-1)^4\pi^4}} = \frac{\alpha_d \left[\frac{1}{8} - \sum_{j=1}^{N-1} \frac{1}{(2j-1)^2\pi^2}\right]}{\frac{1}{24} - \sum_{j=1}^{N-1} \frac{4}{(2j-1)^4\pi^4}} \tag{57}$$

For N=35, (57) can be simplified to

$$\alpha_{m,N} \simeq 34240\ \alpha_d \tag{58}$$

3. Code Architecture

STAMMT-R 1.0 is written in FORTRAN 77 using subroutines from SLATEC (Sandia, Los Alamos, Air Force Weapons Laboratory Technical Exchange Committee) and IMSL (International Mathematics and Statistics Libraries) Version 3.0. The SLATEC routines are distributed with the code because they are in the public domain. However, the IMSL subroutines are proprietary, and can be obtained from Visual Numerics, 9990 Richmond Ave., Suite 400, Houston, TX, 77042-4548, USA; (713)784-3131; marketing@houston.vni.com. On a PC, the code must be compiled with the IMSL library, but may be run without access to the library. On a UNIX workstation, the code must be both compiled and run on a machine with access to an IMSL library and license, respectively.

STAMMT-R is written as a set of subroutines, each of which have a specific function or a specific set of functions. The major subroutines are listed below, with a brief description of the subroutine's function. Some minor subroutines are not described here, including subroutines that are used to set up arrays or subroutines that are used to check on the status of a number (for example, to check if a number is not defined).

All of the subroutines listed below are either part of the IMSL library, or are included with the main program in a single file named **STAMMT-R.f**. Two files (in addition to the IMSL library) are required to compile and run STAMMT-R. The first is **STAMMT-R.f**. The second is an include file named **include.prm**. The parameter values in **include.prm** do not need to be modified, but this file must simply be present in the same directory as **STAMMT-R.f** at the time that the code is compiled. However, some

of the contents of **include.prm** are briefly described below for completeness and to help facilitate any future alterations that may be desired.

For example, it may be desirable in some instances to reduce the value of the parameter **nts** in **include.prm** to match the value of **TNS** (number of concentration data points in SWIW) given in **file 1** of **STAMMT-R.prj** (see Section 4.2.1 of this manual) as this can significantly reduce the run time of the program. Also, if the number of parameters inverted for in a parameter estimation run is less than 5, then (in addition to alterations in the main program and the subroutine **obj**) the value of **nx** in **include.prm** must be changed to the correct value. In parameter estimation runs, it is also best to set **nts** and/or **ntm** in **include.prm** to **TNS** and **TNM**, respectively. The parameter **TNM** is the number of concentration data points in the two-well injection-withdrawal. Note that any change to **include.prm** requires recompilation of the code.

3.1. Program STAMMT-R

This is the main routine of STAMMT-R. The main tasks that this routine is responsible for are the following:

1) Setting up common blocks and most arrays that are used throughout the code.
2) Reading the file names to be used for input and output.
3) Reading all parameters, variables, and code settings to be used by the code.
4) Reading in necessary input values and data.
5) Directing the code to follow one of the four major options available (either single-well or two-well simulation, and either parameter estimation or forward simulation). Each of these has specific requirements that are predominantly set up within the main routine. For example, if estimation is desired, the main routine sets up and initializes required arrays.
6) Calculating the points in time at which a simulated breakthrough curve concentration is desired. This operation is performed only for forward simulation (not for estimation), and only if observed concentration data are not used
7) Calling either the single-well or two-well subroutines to calculate the breakthrough curve desired. In the case of estimation, this is done after the estimation with the estimated parameter set.
8) In the case of estimation, calculating inversion statistics (i.e., RMSE [root mean squared error], covariance matrix, etc.)
9) Printing out results.

3.2. Subroutine dunlsf (IMSL)

This subroutine solves a nonlinear least-squares problem using a modified Levenberg-Marquardt algorithm. We employ this subroutine to estimate the parameters from data obtained in a single-well or two-well test. We estimate five parameters: the mean of the distribution of $\ln(D_d/a^2)$, μ^*; the standard deviation of the distribution of $\ln(D_d/a^2)$, σ; the fracture porosity of the formation, ϕ_f; the dispersivity in the single-well test α_L; and the dispersivity in the two-well test, α_L. When both SWIW and two-well simulations are run, the dispersivity may be different.

3.3. Subroutine obj

This subroutine is called only if the parameter estimation capabilities of STAMMT-R are used. It is called by **dunlsf** (3.2) and calculates the value of the

objective function for a particular set of parameters chosen by **dunlsf**. The objective function is an array of numbers, each containing the difference between the simulated value and the known data value. The simulated values are calculated by **btcalcm** (3.4) and/or **btcalcs** (3.5). The subroutine also prints progress information for the parameter estimation and breakthrough curves to temporary files after every simulation.

3.4. Subroutine btcalcm

This subroutine drives the calculation of the concentration values in the breakthrough curve for a two-well simulation. The mathematics used in this subroutine are described in Section 2.3.

3.5. Subroutine btcalcs

This subroutine drives the calculation of the concentration values in the breakthrough curve for a single-well (injection-withdrawal) simulation. The mathematics used in this subroutine are described in Section 2.2.

3.6. Subroutine dinlap (IMSL)

This subroutine calculates the inverse Laplace transform of a complex function. We use this subroutine to calculate the breakthrough curves within both **btcalcm** (3.4) and **btcalcs** (3.5). This subroutine requires that the solution to a partial differential equation be known in the Laplace domain, and that solution must be coded as a complex function. This subroutine in turn calls one of several other subroutines, depending on the solution required.

3.7. Subroutine dcsint (IMSL)

This subroutine computes the cubic spline interpolants. It is used, in conjunction with **dcsval** (3.9) in finding a continuous function running through a known number of points. This is required at several points within the program.

3.8. Subroutine dcsval (IMSL)

This subroutine evaluates a cubic spline (i.e., computes an interpolated value between points known along a function, based on a cubic spline) given the cubic spline interpolants (3.8).

3.9. Subroutines dqdag, dq2ag (IMSL)

These subroutines integrate a function using a globally adaptive scheme based on Gauss-Kronrod rules. This numerical integration scheme is used at several points within the program for various purposes. The determination of whether to use **dq2ag** or **dqdag** is dependent upon the specific options needed in the integration.

3.10. Subroutine avint (SLATEC)

This subroutine numerically integrates a function when no continuous form of the function is available, but only a number of points along the function.

3.11. Function pushcL

This function calculates the value of the *Laplace-domain-concentrations in the mobile zone for divergent flow in the two-well simulation* (see Section 2.2.1). It does this as a function of the complex Laplace parameter p, and is called by **dinlap**.

3.12. Function pushsL

This function calculates the value of the *Laplace-domain-concentrations in the immobile zone for divergent flow in the two-well simulation* (see Section 2.2.1). It does this as a function of the complex Laplace parameter p, and is called by **dinlap**.

3.13. Function crt

This function contains the integrand, given in equation (43), used for azimuthally averaging the concentrations for the two-well simulation. Azimuthal averaging of concentrations is needed in the two-well simulation after the divergent-flow concentration profile has been calculated and the coordinate transformation is completed (see Section 2.3.2)

3.14. Function pullcL

This function calculates the value of the *Laplace-domain-concentrations in the immobile zone for convergent flow in the two-well simulation* (see Section 2.3.1). It does this as a function of the complex Laplace parameter p, and is called by the IMSL subroutine, **dinlap**.

3.15. Function pushcLs

This function calculates the value of the *Laplace-domain-concentrations in the mobile zone for divergent flow in the single-well simulation* (see Section 2.2.1). It does this as a function of the complex Laplace parameter p, and is called by the IMSL subroutine, **dinlap**.

3.16. Function pushsLs

This function calculates the value of the *Laplace-domain-concentrations in the immobile zone for divergent flow in the single-well simulation* (see Section 2.2.1). It does this as a function of the complex Laplace parameter p, and is called by the IMSL subroutine, **dinlap**.

3.17. Function restcL

This function calculates the value of the *Laplace-domain-concentrations in the mobile zone for the resting phase in the single-well simulation* (see Section 2.2.2). It does this as a function of the complex Laplace parameter p, and is called by the IMSL subroutine, **dinlap**.

3.18. Function restsL

This function calculates the value of the *Laplace-domain-concentrations in the immobile zone for the resting phase in the single-well simulation* (see Section 2.2.2). It

does this as a function of the complex Laplace parameter p, and is called by the IMSL subroutine, **dinlap**.

3.19. Function pullcLs

This function calculates the value of the *Laplace-domain-concentrations in the mobile zone for convergent flow in the single-well simulation* (see Section 2.2.3). It does this as a function of the complex Laplace parameter p, and is called by the IMSL subroutine, **dinlap**.

3.20. Function integR

This function calculates the real part of the integrand from equation (36). It does this for both the single-well and two-well simulations.

3.21. Function integI

This function calculates the imaginary part of the integrand from equation (36). It does this for both the single-well and two-well simulations.

3.22. Subroutines zairy, zbiry (SLATEC)

These subroutines calculate the value of the first and second Airy functions, Ai(x) and Bi(x), respectively. They also calculate the first derivatives of these Airy functions, Ai'(x) and Bi'(x). These subroutines depend on many other subroutines and functions that are internal to the SLATEC routines. These subroutines contain machine constants for many different computers. These lines in the subroutines are all commented out, except for those lines which give the machine constants appropriate for the type of computer on which the code is compiled and run.

3.23. Subroutine calc_mass

This subroutine calculates the total amount of mass contained in the aquifer by integrating under the current concentration profile. Used for concentration profiles only.

3.24. Subroutine massratio

This subroutine calculates the ratio of mass remaining in the aquifer to total mass injected. Used for breakthrough curves only. Calls SLATEC subroutine, **avint**.

3.25. Subroutine mtdef

This subroutine permits STAMMT-R to read from an input file and use a user-defined discrete distribution of first-order mass transfer rate coefficients, rather than the lognormal distribution of diffusion rate coefficients or single-valued diffusion rate coefficient which STAMMT-R normally uses. When using this option, the user is confined to distributions of first-order rate coefficients. However, if the multirate distribution is known that is equivalent to a particular distribution of diffusion rate coefficients, then this restriction is effectively removed. Examples of distributions of first-order rate coefficients that could be used include a gamma distribution, a uniform distribution, an exponential distribution, or some other distribution of the user's choice. Creation of an input file containing such a discretized distribution will generally require a preprocessor.

Alternatively, the subroutine may be altered by the user to directly incorporate mass transfer rate coefficients other than lognormal distributions into the code. To use this subroutine, the user must define the PDF b (α_m). In the subroutine, b (α_m) goes by the notation **bet(nm)** and α_m goes by the notation **alpha(nm)**. The dimension **nm** of both arrays is determined in the file **include.prm**. Note that the code must be recompiled if any of the parameters in **include.prm** are altered. Code modifications and recompilation will require recompletion of the test cases listed in Section 5 if the results of the modified code are to be used in the WIPP decision-making process.

3.26. Subroutine distout

This subroutine calculates and writes to a file distributions of diffusion rate coefficients and block radii, in the form of discretized cumulative density functions (CDF). It does this on the basis of the values of the mean and standard deviation of the natural logarithms of the diffusion rate coefficients; these two parameters are either specified in one of the input files (for a forward simulation; see Section 4) or are calculated by STAMMT-R (for an inverse run). Calls SLATEC subroutine, avint.

3.27. File include.prm

This file simply declares and dimensions a number of variables and parameters used throughout the code. The following is a list of parameters declared and given values in include.prm which the user may wish to adjust. Such adjustment would generally only be desirable or necessary if the parameter estimation capabilities of STAMMT-R are used (refer to the discussion at the beginning of Section 3).

nx number of free parameters in the problem. Currently set to 5 (**mu**, **sig**, **poros**, **alphLs**, **alphLm**); this does not ever have to altered for forward simulations. In an inverse run, should be reduced to the number of parameters being estimated if sensitivity, covariance, and correlation matrices are desired as STAMMT-R output. Reducing **nx** to the number of free parameters greatly reduces CPU time for parameter estimation runs, but its value has no effect on CPU time required for forward runs.

nts maximum number of concentration points in calculated or observed single-well simulation. Currently set to 300. For single-well simulations, reducing this to the value of **TNS** will speed up both forward and inverse runs and should be done in inverse runs.

ntm maximum number of concentration points in calculated or observed two-well simulation. Currently set to 300. For two-well simulations, reducing this to the value of **TNM** will speed up both forward and inverse runs and should be done in inverse runs.

nm number of discrete rate coefficients used to define all distributions. The discretization of the distributions can be increased only at a cost to run-time. Currently set to 35 (see Section 2.4.1. for a brief discussion of the influence of this setting).

4. Code Input and Output Structure

4.1. GENERAL GUIDE TO STAMMT-R INPUT AND OUTPUT

STAMMT-R requires a project file and 4 input files, and generates a variable number of output files. The number of output files created depends on whether both SWIW and two-well runs are performed and whether the parameter estimation capabilities of the software are used. Some of these input and output files may be empty, depending on the options selected. However, all input files must exist, and their names must be specified in the project file (see below). All input and output files are in ASCII format. A detailed description of all STAMMT-R input and output files is given in Section 4.2.

The *project file* (**STAMMT-R.prj**) simply lists the filenames of all input and output files used or created in a STAMMT-R run.

The *input files* may be classified into three categories. The first category is administrative in nature and consists of a single parameter file (**File 1**; see Section 4.2). This input file specifies parameters for the simulation, and should be viewed as the steering wheel of the STAMMT-R automobile. The parameter file includes information about the physical characteristics of the aquifer, details of the tracer experiment the user wishes to simulate, and also allows the user to choose between a number of options with respect to the functions STAMMT-R will perform.

The second category of input file consists of two observed data files (**Files 2** and **3**; see Section 4.2). One contains a measured recovery curve from a single-well tracer test, and the other a measured breakthrough curve from a two-well test. As mentioned above, it is not required for a simulation that these files contain data, although they must exist. For parameter estimation, the appropriate input file(s) must, of course, contain observed time vs. concentration data.

The third category of input consists of a single file providing a user-defined distribution of first-order rate coefficients, if desired (**File 17**; see Section 4.2). This file is generally not used, but provides the user with the option of defining his or her own discrete distribution of mass transfer coefficients. **idef** in the parameter file must be set to 1 to use this option. In STAMMT-R Ver. 1.0, this option may only be used in forward simulations.

The *output files* (**Files 3** to **16**; see Section 4.2) provide a variety of information. The main output files contain listings of concentration as a function of time during convergent flow (i.e., a simulated breakthrough curve). Other files contain concentrations in the mobile zone and various types of immobile zone as a function of distance from the pumping or injection wells, for single and two-well simulations, at the end of the push (divergent), rest, and pull (convergent) periods of the simulation, list calculated multirate mass transfer parameters, give the base ten logarithm of the ratio of mass remaining in the

aquifer to total mass injected as a function of the base ten logarithm of pumping time, provide various statistics if the parameter estimation capabilities of the code are used, and give cumulative density functions for diffusive block size and diffusion rate coefficient.

4.2. INPUT/OUTPUT STRUCTURE

4.2.1. **Project File,** STAMMT-R.prj

This file contains a list of filenames to be used as input and output to STAMMT-R. The user may specify any set of filenames desired, but the files must be given in **STAMMT-R.prj** in the following order:

File 1: input parameter file giving aquifer characteristics and type of STAMMT-R run desired;

File 2: input data file containing breakthrough curve data from two-well experiment;

File 3: input data file containing recovery curve data from single-well experiment;

File 4: output file containing breakthrough curve for two-well STAMMT-R run;

File 5: output file containing recovery curve for single-well STAMMT-R run;

File 6: output file containing all calculated α and β_i and β_{tot};

File 7: output file containing concentrations as a function of radial distance from the injection well at the end of injection for the two-well run;

File 8: output file consisting of **File 7** above, converted to concentrations as a function of radial distance from the extraction well;

File 9: output file containing concentrations as a function of radial distance from the injection well at the end of the resting period for a single run;

File 10: output file containing concentrations as a function of radial distance from the injection well at the end of injection for the single-well run;

File 11 output file containing the base ten logarithm of the ratio of mass remaining in the aquifer to total mass injected as a function of the base ten logarithm of time;

File 12: output file giving progress of parameter estimation routine, containing current estimated values of parameters;

File 13: output file giving progress of parameter estimation routine, containing current estimated values of parameters and breakthrough curve for two-well run;

File 14: output file giving progress of parameter estimation routine, containing current estimated values of parameters and breakthrough curve for single-well run.

File 15: output file containing run statistics and related information, including Jacobian matrix (sensitivity of i^{th} concentration to j^{th} parameter), covariance matrix, correlation coefficient matrix, and eigenvalues of the covariance matrix.

File 16: output file containing discrete values of the cumulative density functions describing the diffusion rate coefficients and block radii.

File 17: input file containing user-defined distribution of first-order mass transfer rate coefficients.

*Note that filenames must be specified in **STAMMT-R.prj** for all the above files, and that all input files must exist, even if they are empty and not used.* However, if any of these input files are not used in a given STAMMT-R run, the appropriate files may be left empty.

4.2.2. Input Files

a) **File 1** in **STAMMT-R.prj**

This file contains parameters which describe the physical nature of the aquifer, test-specific information, or the STAMMT-R options the user wishes to invoke. The parameter files used in the test cases described in Section 5 of this manual are given in Appendices A1, A2, A3 and A4; these should serve as templates to be directly modified by the user. A brief explanation of the parameters is given in these input parameter files, and a more thorough description is given in the following tables. Note that parameters pertaining to the characteristics of a two-well simulation (e.g., **Qin**, **alphLm**) are ignored when a single-well run is specified, but a value for these parameters (any value) must be present in the input file. The same is true for parameters pertaining to the characteristics of a single-well simulation if a two-well simulation is performed; that is, every parameter in this file should be assigned some number, regardless of whether that parameter is actually used. Details of this file are given in Table 1 and its use is more generally described below.

STAMMT-R can perform both forward (simulation) and inverse (parameter estimation) modeling of single-well or two-well tracer experiments. The value of the variable **iest** in the parameter file specifies whether a forward simulation or parameter estimation will be performed. For **iest**=1, only forward modeling will be performed; for **iest**=0, parameter estimation will be performed. Note that only the simulation (forward modeling) capabilities of STAMMT-R have WIPP Quality Assurance test problems. The values of the variables **skipm** and **skips** determine whether a single-well or two-well tracer test is modeled. A value of 0 for **skipm** or **skips** specifies that a two-well or single-well run, respectively, should be simulated; a value of 1 specifies that the two-well or single-well run, respectively, should not be simulated. A value of 0 may be assigned to both **skipm** and **skips**, which would specify that both single-well and two-well simulations should be completed in the same STAMMT-R run.

For a forward modeling run, STAMMT-R does not require input data files containing measured breakthrough curves. However, STAMMT-R does require that times at which it must calculate concentrations be specified in some manner. There are two ways to do this. If a file containing a measured breakthrough curve is available, and setting **SWtime** (for a single-well simulation) or **MWtime** (for a two-well simulation) in the parameter file equal to 0, STAMMT-R will calculate concentrations at the same times at which concentrations are given in the observed data. Alternatively, if **SWtime** or **MWtime** is set equal to 1, STAMMT-R will calculate concentrations at a user-specified time interval, and does not require observed data. In this case, STAMMT-R uses the following algorithm to determine the times at which it will calculate concentrations:

$$t(i) = (To + i * inc) * (1.0 - z) + z * [\exp (i * inc) + To - 1.0] \quad (59)$$

with:

$$\text{inc}=\text{pumpt}/TN \text{ for } z=0 \tag{60}$$

$$\text{inc}=\ln(\text{pumpt})/TN \text{ for } z=1 \tag{61}$$

In the above expressions, *t(i)* is time at the i^{th} time step and *To* is the time at which convergent flow starts (equal to **Trest** + **Timeins** for the single-well case, or **Timein** for the two-well simulation; see Table 1 in Section 4.2.1 for definitions). *z* functions as a switch. If $z = 0$, time will be incremented at a constant interval equal to *inc*. If $z = 1$, a variable time interval will be used, which gives a roughly constant increment in ln(time). The (-1) term that is active in the *t(i)* calculation for $z=1$ is included to ensure that the first point in the breakthrough or recovery curve occurs very near the time at which pumping begins. For a single-well simulation, *z*, *pumpt*, and *TN* are represented in the parameter file by the variables **SWz, SWpumpt,** and **TNS**, respectively. For a two-well simulation, *z*, *pumpt*, and *TN* are represented in the parameter file by **MWz, MWpumpt**, and **TNM**, respectively. Note that if single and two-well simulations are completed in the same STAMMT-R run, it is possible to use an input data file for one of the simulations and a user-prescribed time interval in the other.

Regardless of how the times for concentration calculation and output are determined, the user must specify how many time vs. concentration pairs (i.e., how many data points) are desired in the output. The number of data are specified by the variables **TNS** and/or **TNM** in the parameter file, depending on whether a single-well or two-well simulation (or both) is performed. If times are extracted from an input file by STAMMT-R (i.e., if **SWtime** and/or **MWtime** = 0), **TNS** or **TNM** must be less than or equal to the number of data points in the input file. If times for output are calculated by STAMMT-R at user-specified intervals (i.e., if **SWtime** and/or **MWtime** = 1), then **TNS** or **TNM** may be any number less than 300. This maximum permissible value of 300 data points may be changed by altering the values of **nts** and/or **ntm** in the include file (**include.prm**). However, it must be noted that the include file is part of the STAMMT-R source code. If this file is altered, the code must be fully recompiled and re-tested for Quality Assurance purposes.

When running either a single-well or two-well simulation, it is necessary to specify **rmaxs** or **rmax**, respectively, which is the maximum distance from the injection well at which solute injection will be simulated. As a first approximation, this may be calculated by (using two-well parameters for example only)

$$\mathbf{rmax} = \sqrt{\frac{Q_{in}\left(t_{in} - t_{in}\right)}{\pi b \phi_f} - r_w^2} = \sqrt{\frac{\mathbf{Qin}\left(\mathbf{Tin} - \mathbf{Tc0}\right)}{\pi\, \mathbf{b1}\, \mathbf{poros}} - \mathbf{r0i}^2} \tag{62}$$

It is very important for the user of STAMMT-R to ensure that the simulated injected concentrations are contained within **rmax**. For highest accuracy, it is also important to ensure that **rmax** is not significantly larger than needed. STAMMT-R will

provide a warning if **rmax** is significantly too large or too small, and will indicate which is the case; however, it is prudent to manually verify whether it is set correctly. To check this, it is generally necessary to run the code, and then check the **File 7** (see Section 4.2.1) for a two-well run, or **File 9** for a single-well run. Note that these output files are printed after a small fraction of the total run time, so it is possible to run the code for a short time, then check these files. If **rmax** is set properly, two criteria will be met:

(1) Concentrations will be a small, non-zero percentage of maximum concentrations at the edge of the grid (the bottom (last) concentration entry in the output file). To compare to the maximum concentration, check concentrations near the edge of the well at the top of the file. The bottom (last) concentration in the file should be in the range of 10^{-3} to 10^{-6} of maximum concentration. If the bottom (last) concentration is larger than this, **rmax** should be made larger. If the bottom (last) concentration is smaller than this, **rmax** should be made smaller.

(2) The mass given at the bottom of these same files should be an accurate representation of true mass injected. True mass injected can be calculated by multiplying the injection concentration by the injection rate by the tracer injection time.

Note also that when using parameter estimation mode, it is necessary to check **rmax** *both before and after* the parameter estimation. In the course of parameter estimation, it is likely that the edge of injected concentrations changes, and it is therefore possible that **rmax** could need to be adjusted and the parameter estimation re-run.

In addition, we note that it is always necessary to keep **rmax** smaller than **Ro** (the well separation in the two-well simulation). If **rmax** is required to be larger than **Ro**, this means that the injected solution is injected beyond the pumping well. *In this case, STAMMT-R cannot be used to accurately simulate the breakthrough curve.*

In theory, it would be possible to have the code calculate the optimal value of rmax. However, when using the code in optimization mode, the code would change rmax as a function of the estimated parameters. This could result in spurious results and a non-smooth objective function. As a result, it was decided to keep rmax within the parameter set to be given by the user. When using STAMMT-R in estimation mode, it is best to check the validity of rmax both before and after the estimation procedure. This is necessary to ensure that the chosen value of rmax is still valid for the estimated parameters.

Table 1: Variable Names and Descriptions for Input File 1

Variable Name	Symbol	Units	Range	Narrative
For an explanation of how to set TNM, MWtime, MWz, MWdt, TNS, SWtime, SWz, and SWdt, refer to Section 4.2.2.				
	Two-well Simulation Parameters:			
skipm	none	-	0 or 1	0=do two-well simulation 1=do not do two-well simulation
Tc0	t_o	[T]	≥0	start time of solute injection into aquifer
TcE	t_{end}	[T]	>**Tc0**	elapsed time from **t=0** to end of solute injection
Timein	t_{in}	[T]	>**TcE**	elapsed time from **t=0** to end of chaser injection
Qin	Q	[L^3/T]	>0	injection rate
Qout	Q	[L^3/T]	>0	pumping rate
alphLm	α_L	[L]	>0	longitudinal dispersivity
rmax	r_{max}	[L]	r0i<rmax<Ro	edge of grid
Ro	R_o	[L]	>r0p+rmax	distance from injection to pumping wells
r0i	r_w	[L]	>0	injection well radius
MWtime	none	-	0 or 1	0=use time increments from two-well time vs. concentration input file. 1=use user-specified time increment instead.
MWz	none	-	0 or 1	*if **MWtime** is set to 1:* 0=use constant time interval 1=use variable time interval which provides more evenly spaced data points in natural log space
MWpumpt	none	[T]	>0	elapsed time from **Tin** to end of pumping
TNM	none	-	see Section 4.1	number of data points desired in breakthrough curve
	Single Well Simulation Parameters:			
skips	none	-	0 or 1	0=do single-well simulation 1=do not do single-well simulation
Tc0s	t_o	[T]	≥0	start time of solute injection into aquifer
TcEs	t_{end}	[T]	>**Tc0s**	elapsed time from t=0 to end of solute injection
Timeins	t_{in}	[T]	>**TcEs**	elapsed time from t=0 to end of chaser injection
Trest	t_{rest}	[T]	>**0**	length of resting period; i.e., elapsed time from **Timeins** to end of rest
Qins	Q	[L^3/T]	>0	injection rate
Qouts	Q	[L^3/T]	>0	pumping rate
alphLs	α_L	[L]	>0	longitudinal dispersivity
rmaxs	r_{max}	[L]	>r0p	distance from center of well to edge of grid
SWtime	none	-	0 or 1	0=use time increments from single-well time concentration input file. 1= use user-specified time increment instead
SWz	none	-	0 or 1	*if **SWtime** is set to 1:* 0=use constant time interval 1=use nonconstant time interval which provides evenly spaced data points in log space
SWpumpt	none	[T]	>0	elapsed time from **(Timeins+Trest)** to end of pumping
TNS	none	-	see Section 4.1	number of data points desired in breakthrough curve

Table 1 (con't)

Variable Name	Symbol	Units	Range	Narrative
	Parameters Common to Both Single Well and Two-well Simulations:			
r0p	r_w	[L]	>0	pumping well radius for two-well simulation; the only well radius specified in a single-well simulation
b1	b	[L]	>0	saturated thickness at injection well
b2	b	[L]	>0	saturated thickness at pumping well
Concin	C_o	[M/L^3]	>0	solute concentration in injected mixture; setting **Concin** to 1 is equivalent to normalizing the injected and calculated concentrations by the initial input concentration
poros	ϕ_f	[-]	$0<\phi_f<1$	fracture porosity
pmat	ϕ_m	[-]	$0<\phi_m<1$	matrix porosity (= **poros** multiplied by the capacity coefficient, β_{tot})
mus	μ	[1/T]	$-\infty<\mu<\infty$	mean of $\ln(D_d/a^2)$
sig	σ	[1/T]	>0	standard deviation of $\ln(D_d/a^2)$. If sig = 0, the simulation switches to conventional spherical diffusion.
Rf	R_f	[-]	≥ 1	mobile zone retardation; no retardation if **Rf**=1
ptot	ϕ_{tot}	[-]	$\phi<\phi_{tot}<1$	maximum total porosity (only used in parameter estimation)
Daq	D_o	[L^2/T]	>0	aqueous diffusion coefficient of solute
tort	τ	[-]	$0<\tau<1$	diffusive tortuosity
	Miscellaneous STAMMT-R Software Parameters:			
iest	none	-	0 or 1	1=single or two-well forward simulation only 0=parameter estimation
idef	none	-	0 or 1	0=default distribution of mass transfer parameters 1=user-defined distribution
disc	none	-	-	estimate of the maximum of the real parts of the singularities of the function inverse Laplace transformed by IMSL function DINLAP (called "alpha" in IMSL literature). If unknown, set to .0d0
kmax	none	-	>0	maximum number of function iterations permitted for each T(i) of IMSL function DINLAP (inverse Laplace transform)
relerr	none	-	>0	relative error desired for IMSL function DINLAP (inverse Laplace transform)

b) **File 2** in **STAMMT-R.prj**

This ASCII text file gives time in the first column and corresponding solute concentration data in the second as determined by a two-well experiment. This file is optional. The user may specify a single-well STAMMT-R run (set **skipm** equal to 1 in the parameter file), which does not require two-well data. For a forward run, concentrations may be calculated at the times given in this input data file (set **MWtime** to 0 in the parameter file), or the user may explicitly choose the times at which concentrations are calculated (set **MWtime** to 1 in the parameter file). Note, however, that this input file must exist regardless of the options selected and its name must be specified in the general project file, **STAMMT-R.prj**. If the file is not used, then it may, of course, be left empty. If this file is used, there must be no 0 concentrations at any time. If concentration is identically 0 for any data point in the file, that data point must be removed. No headers, etc. may be present in the file - only data.

c) **File 3** in **STAMMT-R.prj**

Similar to **File 2** above, except that the breakthrough curve is from a single-well experiment. This file may be left empty if a single-well forward run is selected and **SWtime** is set to 1 in the parameter file, or if only a two-well run is selected, but the file must exist and its filename must be given in **STAMMT-R.prj**. If this file is used, there must be no zero concentration points in it. If concentration is identically 0 at any time, that time-concentration pair must be removed from the data file. No headers, etc. may be present in the file - only data.

d) **File 17** in **STAMMT-R.prj**

This file is only read if **idef** in **File 1** above is set to 1. If **idef** is set to 0, a lognormal distribution of *diffusion* rate coefficients is used by STAMMT-R, which is defined by **mu** and **sig** as set in **File 1** above (or estimated if STAMMT-R parameter estimation capabilities are used). This is the default for STAMMT-R. If **idef** is set to 1, a discrete distribution of *first-order* rate coefficients is read from **File 17** instead; in this case, the values given for **mu** and **sig** in **File 1** are ignored (but must still be given some arbitrary value in the input file). The first column of **File 17** consists of values of the first-order rate coefficients, alpha(i). The second column consists of the corresponding capacity coefficients, beta(i), for each of these immobile zones. The discrete distribution may consist of up to 35 individual rates. Note that 35 rows must be present in this file; if less than 35 rates are desired, pad the remaining rows with nonzero values of alpha(i) and zero values of beta(i).

4.2.3. Output Files

a) **File 4** in **STAMMT-R.prj**

Calculated concentration as a function of time at the extraction well of a two well system during extraction (the "pull" or "convergent" phase of the run). A file is created by STAMMT-R regardless of the run parameters set in the parameter file, but this file will be empty if only a single-well run is selected.

b) **File 5** in **STAMMT-R.prj**

Calculated concentration as a function of time at the well in a single-well STAMMT-R run during extraction (the "pull" or "convergent" phase of the run). A file is created by STAMMT-R regardless of the run parameters set in the parameter file, but this file will be empty if only a two-well run is selected.

c) **File 6** in **STAMMT-R.prj**

Three-column file consisting of alpha(i) (rate coefficients), beta(i) (a measure of the lognormal distribution of rate coefficients), and cumulative beta(i) for all i, i=1 to 35; see Section 2. The last (bottom) entry in the third column is the capacity coefficient, a measure of the ratio between mass in the immobile and mobile zones. This file will be created, and contain information, for all STAMMT-R runs.

d) **File 7** in **STAMMT-R.prj**

Concentrations in the mobile zone and 4 types of immobile zone as a function of radial distance from the injection well at the end of injection for the two-well run. If a single-well run is selected (i.e., **skipm** set equal to 1 in parameter file), this file will be created but it will be empty.

e) **File 8** in **STAMMT-R.prj**

File 7 above, converted to concentrations as a function of radial distance from the extraction well. Again, this file will be created by STAMMT-R but will be empty if only a single-well run is selected in the parameter file.

f) **File 9** in **STAMMT-R.prj**

Concentrations as a function of radial distance from the injection well at the end of the resting period for the single-well run. Concentrations are again given for the mobile zone and 4 types of immobile zone. This file will be created but empty for two-well-only runs.

g) **File 10** in **STAMMT-R.prj**

Concentrations in the mobile zone and 4 types of immobile zone as a function of radial distance from the injection well at the end of injection for the single-well run. The file will be created but empty for two-well-only runs.

h) **File 11** in **STAMMT-R.prj**

Output file containing the base ten logarithm of the ratio of mass remaining in the aquifer to total mass injected, given as a function of the base ten logarithm of time elapsed since the start of pumping. The ratio of M/M_0 is calculated as a function of time. The procedure sets M equal to the integral of the single-well breakthrough curve from the start of pumping to the time at which the ratio is evaluated, multiplied by **Qouts**; and Mo equal to the mass in the aquifer at the end of the rest phase, as given at the bottom of **File 9** of **STAMMT-R.prj**. This file is created for both single-well and two-well runs, but will be empty if only a two-well simulation is performed. ***Note:*** as much of the tracer mass in the aquifer is removed by advective transport close to the start of pumping, the results listed in this file are unlikely to be accurate unless the time of the first observation is close

to the start of pumping and the sampling rate is high at small times following the start of pumping. These parameters are set either by the data in **File 3** of **STAMMT-R.prj** or by the selection of **TNS** in **File 1** of **STAMMT-R.prj** (see Section 4.1).

i) **File 12** in **STAMMT-R.prj**

Lists β_{tot} (the ratio of matrix porosity to fracture porosity), μ, σ, ϕ_f, and α_L for both two well and single-well models (**alphLm** and **alphLs**, respectively), at intervals during the inversion process. This file will only be created if parameter estimation is performed (if **iest**=1).

j) **File 13** in **STAMMT-R.prj**

Lists β_{tot} (the ratio of matrix porosity to fracture porosity), μ, σ, ϕ_f, and α_L for the two-well model (**alphLm**), along with the two-well breakthrough curve, at intervals during the inversion process. This file will only be created if parameter estimation is performed (if **iest**=1).

k) **File 14** in **STAMMT-R.prj**

Lists β_{tot} (the ratio of matrix porosity to fracture porosity), μ, σ, ϕ_f, and α_L for the single-well model (**alphLs**), along with the single-well breakthrough curve, at intervals during the inversion process. This file will only be created if parameter estimation is performed (if **iest**=1).

l) **File 15** in **STAMMT_R.prj**

Output file giving parameter estimation statistics. File will be empty unless parameter estimation is performed. This file contains the following: **(1) The Jacobian (sensitivity matrix).** This is a nts (for single-well only), ntm (for two-well only), or nt (for simultaneous single./two-well inversion) by nx matrix giving the derivative of concentration with respect to the estimated parameter as a function of time. That is, time increases down the matrix, each column represents one of the parameters which are estimated by the inversion, and the entries show how a minor perturbation in the estimated value of each of those parameters will affect concentration. Note that as far as the parameter estimation routine and statistics are concerned, the parameters estimated are mus, and the natural logarithms for any other parameters (e.g., sig, alphLs, poros). **(2) square of the Jacobian (information matrix). (3) Covariance matrix**. For a SWIW-only or two-well only parameter estimation run, this nx by nx matrix is equal to the inverse of the information matrix, multiplied by the variance in the data. We assume that data errors are uncorrelated and that residuals are due to measurement rather than model error, and thus use $(RMSE)^2$ as a measure of variance. The diagonals of this matrix give an estimate for the variance (i.e., a measure of uncertainty) for the values of each of the parameters estimated. For a simultaneous SWIW/two-well inversion, the details of the calculation are altered very slightly but the assumptions remain the same. **(4) Correlation coefficients**, an nx by nx matrix giving a measure of the linear correlation between the parameters estimated. An entry of 1 indicates perfect linear correlation. This is a useful and concise summary statistic, but should generally not be used without taking a look at a plot of the Jacobian first. **(5) Eigenvalues of the covariance matrix.**

The ratio of the largest to the smallest eigenvalue is the condition number of the covariance matrix, and gives a statistical indication of the estimability of the problem: the smaller the condition number, the more reliable the result.

m) **File 16 in STAMMT-R.prj**

Output file giving distributions of block sizes and diffusion rate coefficients. File is created for all STAMMT-R runs, but computations performed only for any STAMMT-R forward or inverse run with a value of sig > 0.01 (i.e., for all multirate diffusion runs). 1st and 3rd columns list regularly-spaced values of block radius and diffusion rate coefficient, respectively; 2nd and 4th columns give corresponding cumulative distribution functions, evaluated for those values of block radii and diffusion rate coefficients, respectively.

4.3. Messages to the User

STAMMT-R provides a small number of error and information messages to the user. Error messages are briefly explained here, followed by information messages, in the order that they occur in the code. All messages are printed to the screen.

4.3.1. Error Messages

(1) ERROR: TNS is greater than nts (nominally 300)
Modify TNS, or recompile (and re-QA) with larger nts
Aborting STAMMT-R run

This error message indicates that the number of data given for SWIW in File1 is greater than dimensions of code. The only solutions are to reduce the number of data or to redimension the code (however, redimensioning requires that certain QA procedures must be repeated before the code is run again).

(2) ERROR: TNM is greater than ntm (nominally 300)
Modify TNM, or recompile (and re-QA) with larger ntm
Aborting STAMMT-R run'

This error message indicates that the number of data given for TWIW in File1 is greater than dimensions of code. The only solutions are to reduce the number of data or to redimension the code (however, redimensioning requires that certain QA procedures must be repeated before the code is run again).

(3) ERROR: first time in 2-well data is < Timein
Aborting run
Modify data and/or input parameter files

This error message indicates that the first time in TWIW data set is before injection ends at the injection well. In this case, the conditions discussed in Section 2.3.1. are violated. Parameters must be modified to meet these conditions. If this is not possible, it is necessary to use a code other than STAMMT-R.

(4) ERROR: first time in SW data is < Tins+Trest
Aborting run'
Modify data and/or input parameter files

This error message indicates that the first time in SWIW data set is before the end of rest period. In theory, any data before the end of the rest period should be zero and therefore may be deleted.

(5) ERROR: rmax for multiwell simulation is too large

This error message indicates that rmax is too large for the TWIW simulation. Reduce the value of rmax.

(6) ERROR: rmax for multiwell simulation is too small

This error message indicates that rmax is too small for the TWIW simulation. Increase the value of rmax.

(7) ERROR: rmaxs for SWIW simulation is too large

This error message indicates that rmax is too large for the SWIW simulation. Reduce the value of rmax.

(8) ERROR: rmaxs for SWIW simulation is too small

This error message indicates that rmax is too small for the SWIW simulation. Increase the value of rmax.

(9) icbar gt dcb in pushcL. Increase dcb

This error message indicates that the vector size dcb is not large enough to save the Laplace-domain concentrations (used in calculating the immobile-domain concentrations without having to recalculate the mobile-domain concentrations). In general, this error will occur when the routine is having convergence problems. In this case, there may be other problems with the run (incorrect input parameters, or input parameters that the code cannot handle - see Section 6). Note that an increase in dcb requires recompiling the code.

(10) icbar gt dcb in restcL. Increase dcb

This error message indicates that the vector size dcb is not large enough to save the Laplace-domain concentrations (used in calculating the immobile-domain concentrations without having to recalculate the mobile-domain concentrations). In general, this error will occur when the routine is having convergence problems. In this case, there may be other problems with the run (incorrect input parameters, or

input parameters that the code cannot handle - see Section 6). Note that an increase in dcb requires recompiling the code.

4.3.2. Informational Messages

(1) Done injection for multiwell simulation

This message is printed to the screen when the injection period of the two-well simulation is completed.

(2) Starting pumping for multiwell simulation

This message is printed to the screen when the pumping period of the two-well simulation is completed.

(3) Done injection for Single-Well Injection/Withdrawal

This message is printed to the screen when the injection period of the SWIW simulation is completed.

(4) Done resting period for SWIW

This message is printed to the screen when the resting period of the SWIW simulation is completed.

(5) Starting pumping for SWIW

This message is printed to the screen when the pumping period of the SWIW simulation is initiated.

5. Verification Test Problems

The accuracy of STAMMT-R forward modeling output was tested with four problems and five sets of calculations. Verification Problems 1 and 3 are comparisons of STAMMT-R flow and transport results to those of the SWIFT II code [*Reeves et al.*, 1986] (SWIFT II ver. 2F WPO#21506), for single-well and two-well simulations, respectively. Verification Problem 2 is a comparison of mass transfer predicted by STAMMT-R to that given by the analytical solution of *Haggerty* [1995]. Input parameter files (File 1 of Section 4.2.2.) for Verification Problems 1, 2, 3, and 4 are given in Appendices A1, A2, A3, and A4, respectively.

5.1. Verification Problem 1: Flow and Transport, Single Well Case

The code is verified for a single-well injection-withdrawal test by running the code for the parameters listed below and comparing the results to those given by the SWIFT II code [*Reeves et al.*, 1986]. **The feature of the model that is verified in Problem 1 is the advection-dispersion-mass transfer accuracy for a single-well injection-**

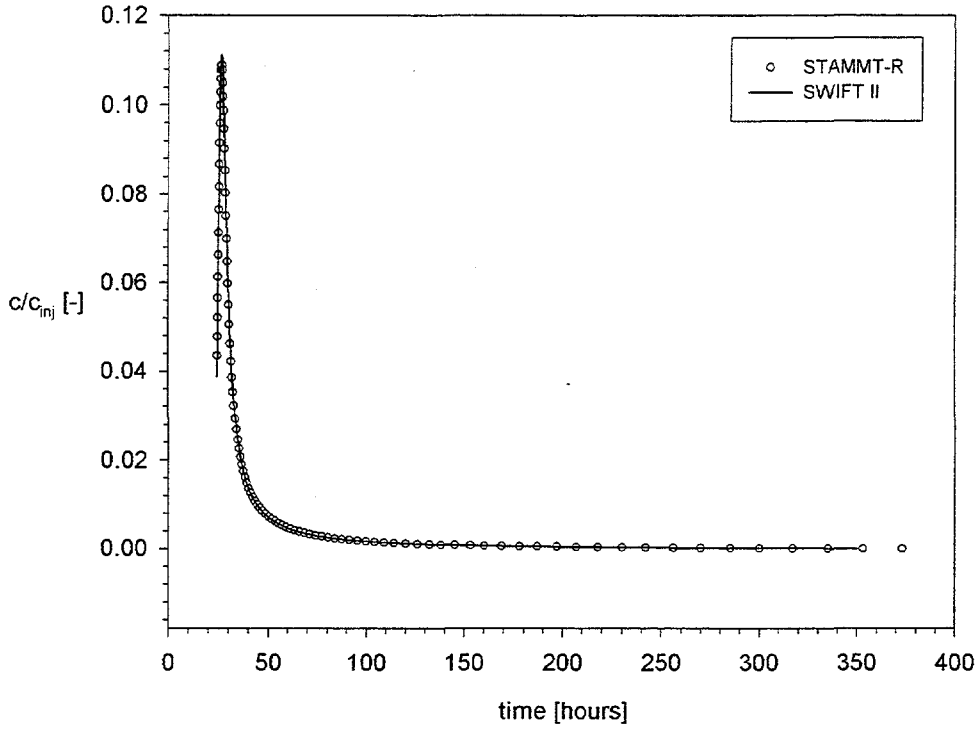

Figure 4: Verification Problem 1. Test of accuracy SWIW solution, shown in arithmetic space. STAMMT-R vs. SWIFT II.

withdrawal test and diffusion into spherical immobile zones. Since SWIFT II can only simulate a single diffusion rate coefficient, the variability of the rate coefficient is set to 0. Plots of the breakthrough curves produced by STAMMT-R and SWIFT II are given in Figures 4 and 5.

The acceptance criterion is an excellent quality of fit of the breakthrough curve produced by STAMMT-R to that produced by SWIFT II, upon visual inspection of log-space plots of these curves, for points in the curves with c/c_{inj} greater than approximately 10^{-8}.

The input parameter file used is given in Appendix A1.

- dispersivity = 0.10 m
- well radius = 0.098425 m
- mobile-zone retardation factor = 1.0 (i.e., no retardation)
- injection rate = 0.4665 m^3/hr
- pumping rate = 0.8516 m^3/hr

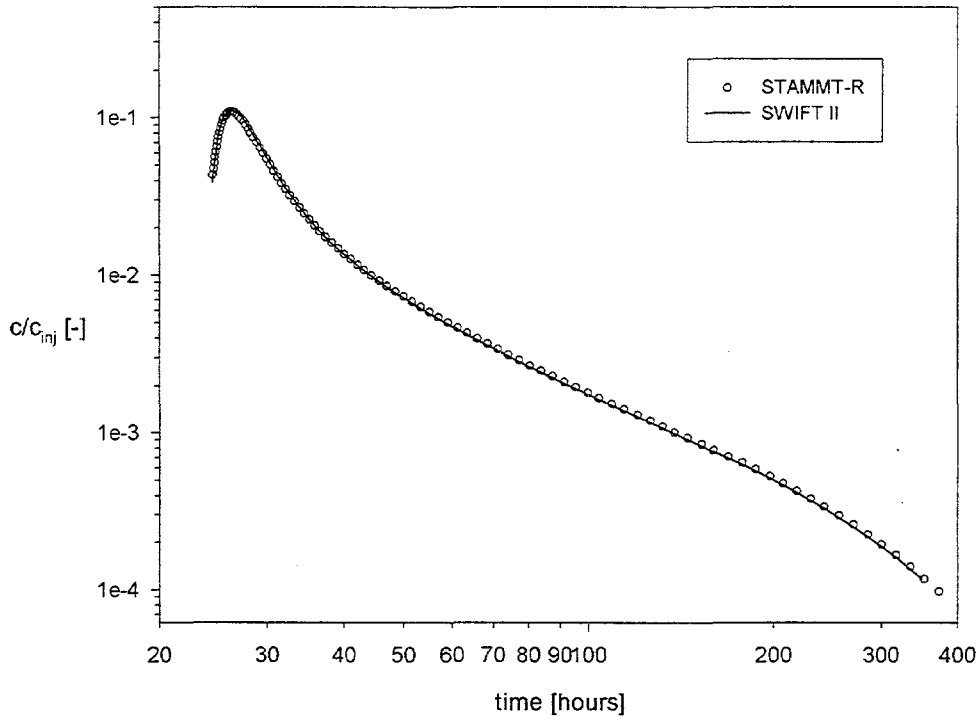

Figure 5: Verification Problem 1. Test of accuracy SWIW solution, shown in logarithmic space. STAMMT-R vs. SWIFT II.

- fracture porosity = 0.05
- thickness of the formation = 7.41 m
- injection concentration = 1.0
- Begin tracer injection at 0.1333 hr
- End tracer injection at 2.25 hr (and begin chaser)
- End chaser injection at 6.633 hr
- resting time = 17.75 hr
- matrix porosity = 0.15
- Free-water diffusion coefficient = $D_w = 7.4 \times 10^{-10}$ m^2/s = 2.664×10^{-6} m^2/hr (needed in SWIFT II [*Reeves et al.*, 1986] only).
- Tortuosity = 0.1 (SWIFT II only).
- Sphere radius (1/2 block size) = 0.01632 m = 1.632 cm (SWIFT II only)
- From the above numbers, $D_w\tau/a^2 = 1 \times 10^{-3}$ hr^{-1} - for STAMMT-R runs this will mean you must set μ^* to $\ln(10^{-3}) = -6.9078$ and set σ to 0.

- Set rmax such that the smallest resulting injected concentration ~ 10^{-6}. (This is the edge of the spatial grid for STAMMT-R - not relevant for SWIFT II).

Figures 4 and 5 show excellent agreement between STAMMT-R and SWIFT II, and the verification is successful.

5.2. Verification Problem 2: Mass Transfer, Single Well Case

The code is verified for a distribution of diffusion rate coefficients (D_a/a^2) by running the code on a given problem (below) and comparing the results to the analytic solution produced by *Haggerty* [1995]. **The feature of the model that is verified with Problem 2 is the mass transfer accuracy for a distribution of diffusion rate coefficients**. A plot of the ratio of mass remaining in the aquifer to the total mass injected as a function of time is given in Figure 6, with the appropriate type curve from *Haggerty* [1995].

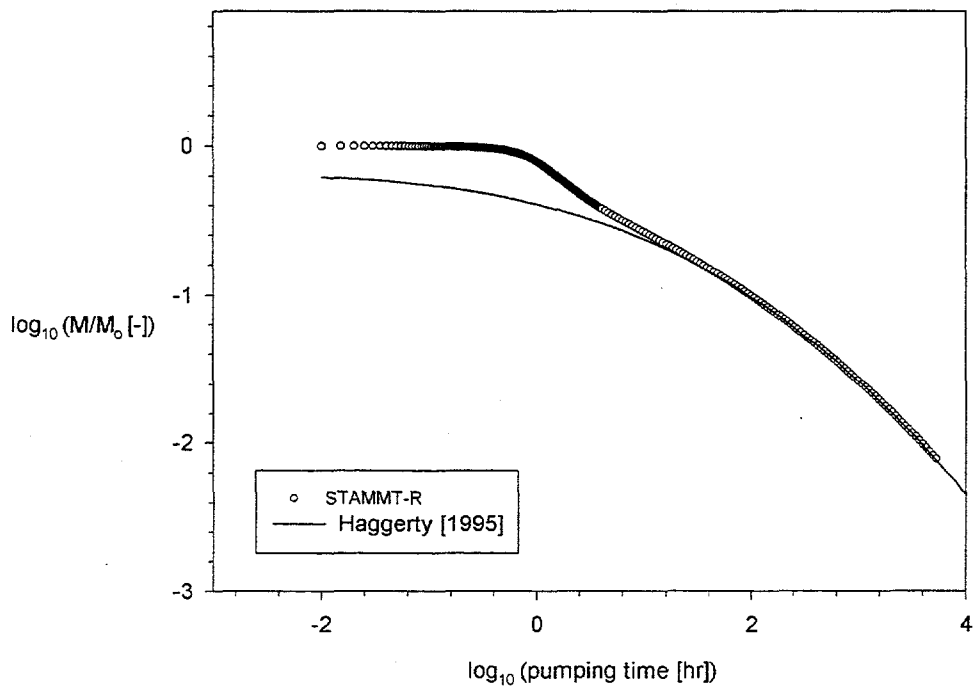

Figure 6: Verification Problem 2. Test of accuracy of multirate mass transfer for a distribution of diffusion rate coefficients. STAMMT-R vs. *Haggerty* [1995]. Note that only late-time solutions should match (as shown).

The acceptance criterion is an excellent quality of fit of the STAMMT-R mass recovery curve to that of *Haggerty* [1995] upon visual inspection of the log-space plots, for the region of the recovery curve dominated by multirate diffusive mass transfer. The type curves of *Haggerty* [1995, p. 198] represent diffusive mass transfer with an exterior boundary condition of zero concentration. For a problem (such as our validation problem), this condition is well-approximated once mass transfer is the dominant rate-limiting process for mass removal from the system. Mass transfer becomes dominant after several pore volumes have been flushed from the medium. In the case of our validation example, ten pore volumes are flushed after 10 hr of pumping. Therefore, mass transfer dominates the system after approximately 10 hr of pumping.

The input parameter file used is given in Appendix A2.

- dispersivity = 0.1 m
- well radius = 0.10 m
- mobile-zone retardation factor = 1.0
- injection rate = 1 m^3/hr
- pumping rate = 10 m^3/hr
- fracture porosity = 0.05
- thickness of the formation = 1.0 m
- injection concentration = 1.0
- Begin tracer injection at 0. hr
- End tracer injection at 10 hr (and begin chaser)
- End chaser injection at 10 hr
- resting time = 10^8 hr (or as long as needed such that all immobile zones are in equilibrium)
- matrix porosity = 0.10
- $\mu^* = -3.0$
- $\sigma = 3.0$
- Set rmax such that the smallest resulting injected concentration ~ 10^{-6}.

Figure 6 shows excellent agreement between STAMMT-R and *Haggerty* [1995] at late time (where the agreement is expected), and the verification is successful.

5.3. Verification Problem 3: Flow and Transport, Two Well Case

The code is verified for a two-well test by running the code on a given problem (below) and comparing the results to those produced by SWIFT II [*Reeves et al.*, 1986]. **The feature of the model that is verified in Problem 3 is the advection-dispersion-mass transfer accuracy for a two-well injection-withdrawal test**. Since SWIFT II can only simulate a single diffusion rate coefficient, the variability of the rate coefficient is set to 0. Plots of the breakthrough curves predicted by STAMMT-R and SWIFT II are given in Figures 7 and 8.

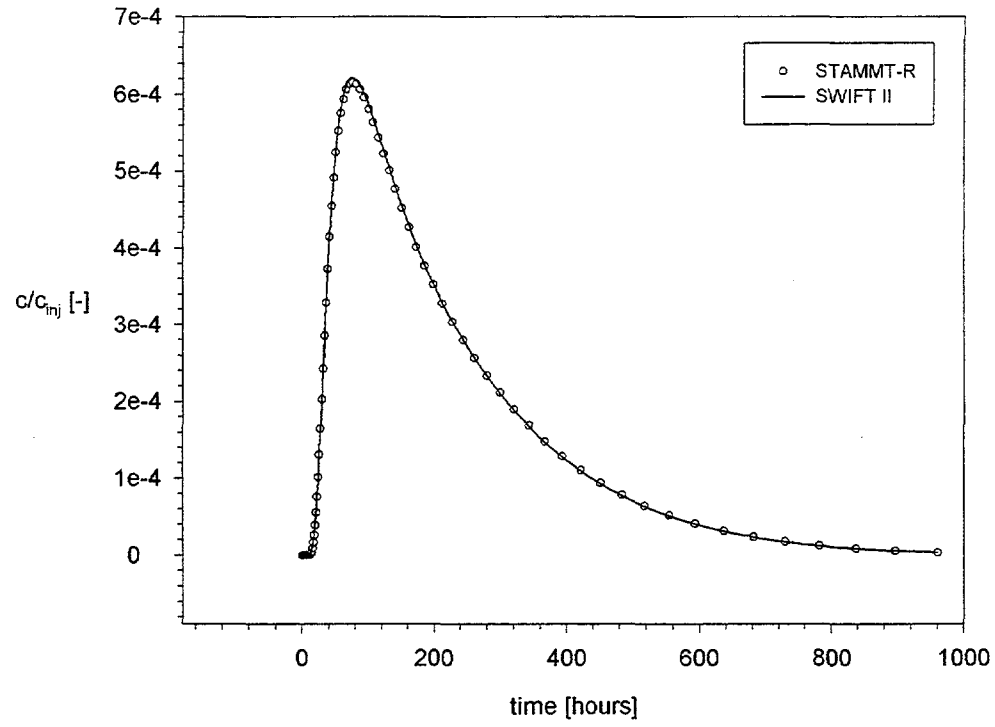

Figure 7: Verification Problem 3. Test of accuracy two-well injection-withdrawal solution, shown in arithmetic space. STAMMT-R vs. SWIFT II.

The criterion for acceptance is a reasonably good match of the STAMMT-R breakthrough curve to that from SWIFT II before the peak concentration, and an excellent match to the SWIFT II results at late times. Goodness of fit is based upon visual inspection of the breakthrough curves as plotted in log-space, for c/c_{inj} greater than approximately 10^{-8}. Early-time concentrations are not expected to match to SWIFT II because the assumptions used by STAMMT-R for the two-well test. Primarily, STAMMT-R assumes that during the tracer injection, the flow field near the pumping well does not affect the flow field near the injection well. In fact, some of the tracer is drawn toward the pumping well during injection. Therefore, the early-time breakthroughs produced by STAMMT-R have lower concentrations than SWIFT II, which does not ignore the pumping well during injection.

The input parameter file used is given in Appendix A3.

- dispersivity = 0.10 m
- injection well radius = 0.10 m
- pumping well radius = 0.10 m

- mobile-zone retardation factor = 1.0
- injection rate = 0.5 m^3/hr
- pumping rate = 1 m^3/hr
- fracture porosity = 0.01
- thickness of the formation = 4.0 m
- injection concentration = 1.0
- Begin tracer injection at 0 hr
- End tracer injection at 0.3 hr (and begin chaser)
- End chaser injection at 0.5 hr
- matrix porosity = 0.16
- distance from injection to pumping well = 10 m
- Free-water diffusion coefficient = $D_w = 7.4 \times 10^{-10}$ $m^2/s = 2.664 \times 10^{-6}$ m^2/hr (needed for SWIFT II [*Reeves et al.*, 1986] only).
- Tortuosity = 0.1 (SWIFT II only).
- Sphere radius (1/2 block size) = 0.01632 m = 1.632 cm (SWIFT II only)

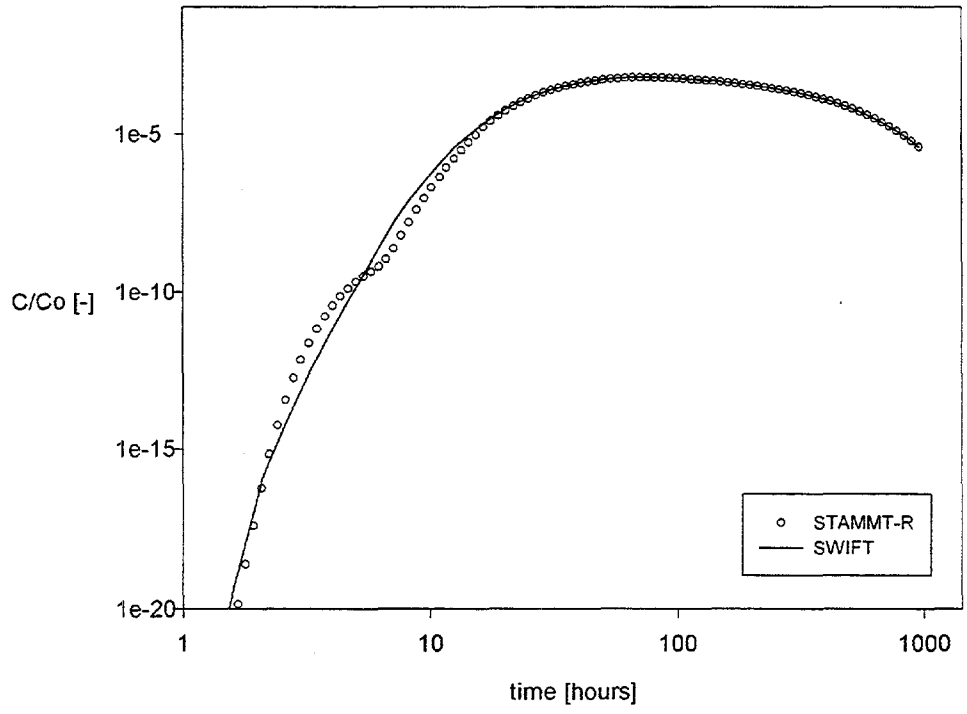

Figure 8: Verification Problem 3. Test of accuracy two-well injection-withdrawal solution, shown in logarithmic space. STAMMT-R vs. SWIFT II.

- From the above numbers, $D_w\tau/a^2 = 1 \times 10^{-3}$ hr^{-1} - for STAMMT-R runs this will mean you must set μ^* to $\ln(10^{-3}) = -6.9078$ and set σ to 0.
- Set rmax such that the smallest resulting injected concentration ~ 10^{-6}. (This is the edge of the spatial grid for STAMMT-R - not relevant for SWIFT II).

Figures 7 and 8 show excellent agreement between STAMMT-R and SWIFT, and the verification is successful.

5.4. Verification Problem 4: Flow and Transport, Single Well Case

The features of the model that are verified in Verification Problem 4 are the STAMMT-R code's ability to do the following: (1) generate a synthetic recovery curve using a constant, user-determined time increment; (2) use a user-defined distribution of first-order mass transfer rate coefficients as input; and (3) produce a CDF of diffusion rate coefficients as output.

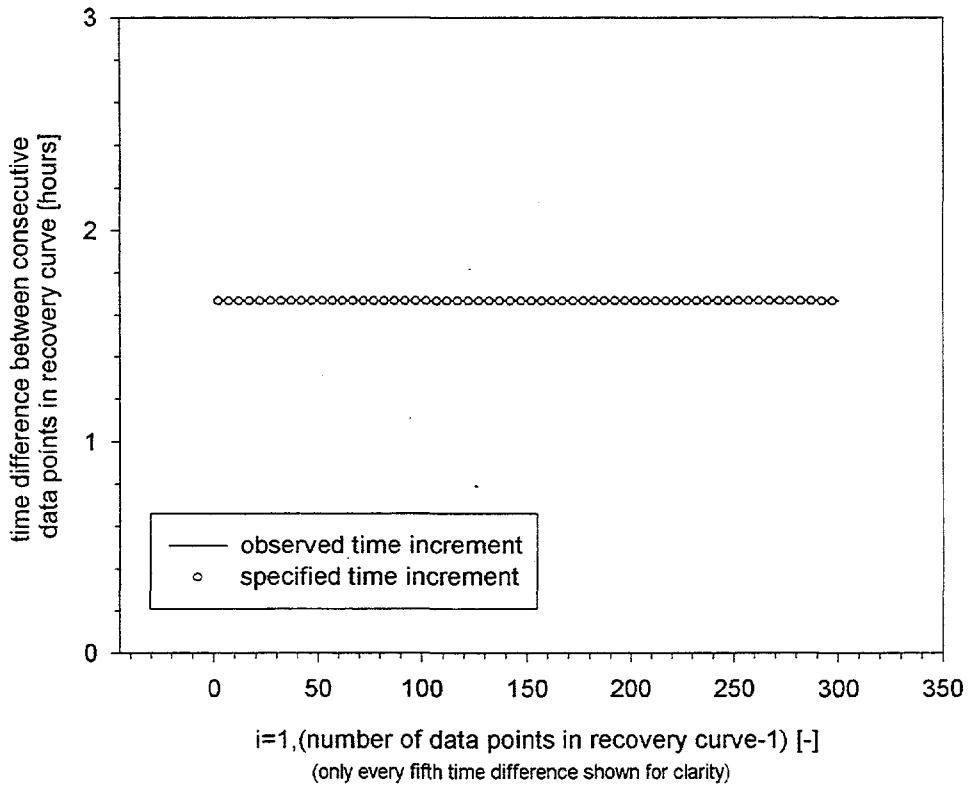

Figure 9: Verification Problem 4. Test of time incrementation specified in input file vs. time incrementation observed in output file.

The first issue is addressed by comparing the spacing between data points in the recovery curve produced by STAMMT-R to that specified in the input file, *QA4A.prm*, equal to **SWpumpt/TNS**. The difference between times in subsequent points in the recovery curve is determined for all data points in the recovery curve and compared to **SWpumpt/TNS** (Figure 9). The criterion for acceptance is that this difference is precisely equal to **SWpumpt/TNS** over the breakthrough curve.

Second, the ability of STAMMT-R to use a user-defined distribution of first-order rate coefficients is shown by comparing the recovery curve predicted by STAMMT-R for a lognormal distribution of diffusion rate coefficients to that predicted by STAMMT-R for an equivalent discrete distribution of first-order rate coefficients. The criterion for acceptance is that two recovery curves must appear identical, upon visual inspection, when plotted graphically in log-space (Figure 10), for points in the breakthrough curve at which c/c_{inj} is greater than approximately 10^{-8}.

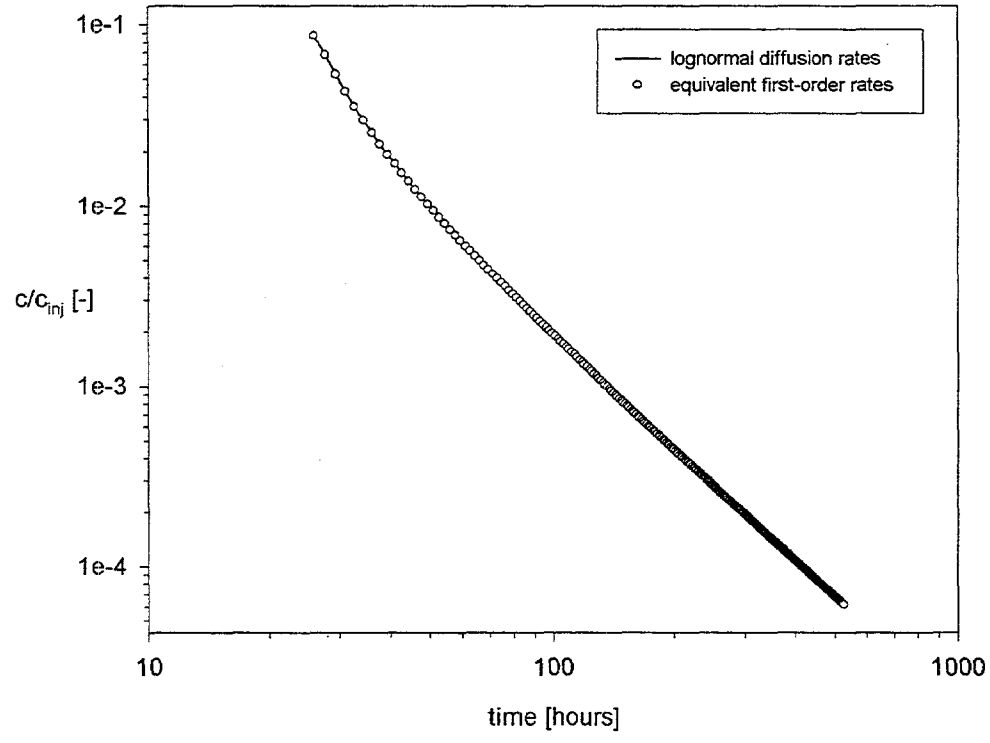

Figure 10: Verification Problem 4. Test of concentration output for lognormal distribution of diffusion rate coefficients vs. equivalent distribution of first-order rate coefficients [*Haggerty and Gorelick*, 1998].

Third, STAMMT-R must correctly produce a CDF of diffusion rate coefficients when requested. The acceptance criterion is that the CDF of diffusion rate coefficients given as output by STAMMT-R using a lognormal distribution of diffusion rate coefficients, and a CDF with an identical geometric mean and standard deviation calculated using a spreadsheet program (Microsoft Excel for Windows 95 Version 7.0a), must show a similar form, upon visual inspection, when plotted graphically (Figure 11). As the numerical integration completed using Excel is crude, a perfect match in Figure 11 is not expected. The procedure and parameters used in Verification Problem 4 are given below.

This verification problem consists of two individual *STAMMT-R* runs. The first only requires a single input file, *QA4A.prm* (given in Appendix A4). The values of the input parameters in this first run of Validation Problem 4 are arbitrarily selected, with the exception of the parameters **idef, SWtime, SWz, SWpumpt,** and **TNS**. **idef** is set to a value of 0, so that *STAMMT-R* uses a lognormal distribution of diffusion rate coefficients in its calculations, using the values of the geometric mean and standard deviation of that lognormal distribution as specified in the input file. **Swtime** is set to 1, so that a user-

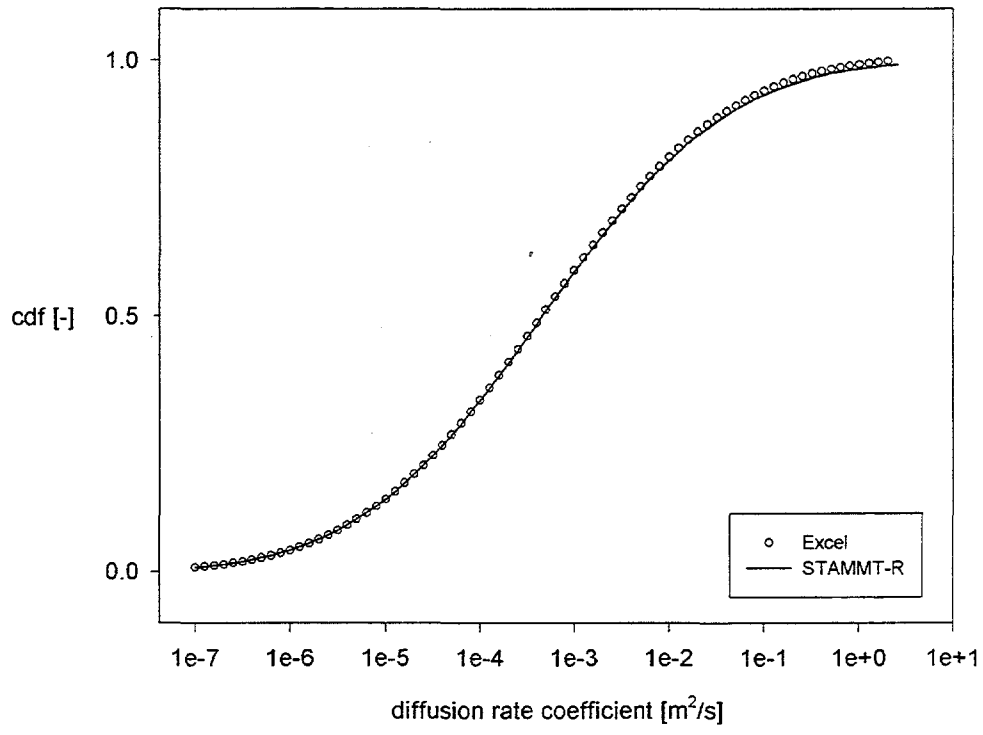

Figure 11: Verification Problem 4. Test of distribution (CDF) of diffusion rate coefficients generated by STAMMT-R vs. that generated with Microsoft Excel.

defined time increment in the recovery curve is used. **SWz** is set to 0, so that a linear time increment is used. The values of **SWpumpt** (duration of pumping) and **TNS** (number of data points in recovery curve) are arbitrary, but the value of **SWpumpt/TNS** gives the length of the time increment which we wish to check against the output file.

An output file from this run, *QA4A.mt*, contains a discrete distribution of first-order mass transfer rate coefficients. The *STAMMT-R* code's ability to convert a continuous lognormal distribution of diffusion rate coefficients into a discrete distribution of first-order rate coefficients is effectively tested by Verification Problems 1, 2, and 3.

The output file *QA4A.mt* is then converted into an input file for the second *STAMMT-R* run in this validation problem. This is done by removing the header and third column from *QA4A.mt* and renaming it *QA4B.dst*. *QA4B.dst* is also given in Appendix A4. The input parameter file for this second *STAMMT-R* run is identical to that of the first, except that the value of **idef** is changed to 1, so the *STAMMT-R* code will use the discrete distribution of first-order mass transfer rate coefficients specified in *QA4B.dst*. The input parameter file is named *QA4B.prm*, and is also given in Appendix A4.

Figures 9, 10, and 11 show that STAMMT-R makes the required calculations correctly, and verification is successful.

6. STAMMT-R Limitations

The applicability of STAMMT-R is limited by the validity of the following assumptions, which are also discussed in Section 2: (1) the aquifer is homogeneous at the macroscopic scale (beyond the representative elementary volume, or REV) for all parameters controlling both flow and transport; (2) there is no regional gradient; (3) mass transfer is dominated by diffusion into and out of immobile zones; (4) if diffusional mass transfer is used, the diffusion rate coefficient, D_e/a^2, is either lognormally distributed or is single-valued (conventional spherical matrix diffusion). Departures from these assumptions may not significantly influence the reliability of STAMMT-R results, but the user must bear these limitations in mind when using the code and, as always, use his or her professional judgment when interpreting the results.

There are four known difficulties that may be encountered when using STAMMT-R for certain sets of physical parameters. These difficulties are of little or no consequence in simulations for which the code was designed: however, users wishing to use STAMMT-R for other purposes should be aware of this limitation. The first difficulty occurs if the value given in **File 1** of **STAMMT-R.prj** for the chaser injection duration is very small, on the order of about 3% or less of injection time (i.e., if **Timeins** or **Timein** is almost equal to **TcEs** or **TcE,** respectively). In this case, the STAMMT-R solution may not converge. This difficulty is not of any significance to the WIPP project, as these parameter sets are not encountered in modeling the field-scale tracer tests conducted in the Culebra dolomite.

The second difficulty arises when the value given in **File 1** of **STAMMT-R.prj** for diffusive porosity (**pmat**) is very small, as this reduces the value of the total capacity coefficient to a very small number. The extent to which this is a problem depends in part on the values of other parameters; for example, a larger dispersivity partially offsets this effect. Some numerical error in the one or two of the lowest concentrations (at the outer edge of the spatial grid) in some of the immobile zones may occur for **pmat** ~ 0.015. More substantial difficulties may occur for much smaller values of **pmat** (~ 0.00005) and a small **alphLs** relative to the advective travel distance, and STAMMT-R will not run for **pmat** = 0 regardless of the value given for dispersivity. It should be noted that diffusive mass transfer will be negligible for such small values of matrix porosity. This second difficulty is not of any significance to the WIPP project, as these parameter sets are not encountered in modeling the field-scale tracer tests conducted in the Culebra dolomite.

The third difficulty involves the inaccuracy of STAMMT-R for the very specific case of (1) very large block sizes; (2) large β_{tot} (i.e., large matrix-to-fracture porosity ratio); (3) short travel times; and (4) single-rate mass transfer. If you change any one of the 4 conditions the problem will disappear or be very minimal. The consequence of this specific combination of circumstances and parameters is that the early-time breakthrough curve is inaccurate (the late-time breakthrough curve is accurate, however). The inaccuracy causes the very earliest breakthrough (at or before the advective time-scale) concentrations to be larger than they should be, while concentrations after the advective time-scale (after the peak) are slightly smaller than they should be. The result is a non-smooth mass recovery curve when the true mass recovery curve is quite smooth. For the WIPP-specific single-well injection-withdrawal first-breakthrough-time of approximately 24 hr, this is only a problem if the single-rate half-block size is greater than approximately 0.5 m. For a further discussion of this difficulty, see Section 2.4.1.

The fourth difficulty lies in the simulation of SWIW breakthrough curves for very early times. STAMMT-R has difficulty converging to a solution if the requested simulation times result in simulated concentrations that are far below the peak concentration. The difficulty results in STAMMT-R taking very long times to run. For this reason, it is suggested that preliminary simulations not request simulation times too close to the turning on of the pump. Once the time of the peak concentration is known, it is suggested that simulation times before the peak be held as close to the peak as possible. STAMMT-R should not have a problem simulating pre-peak c/c_{inj} concentrations of greater than 10^{-5}. Simulation times resulting in pre-peak c/c_{inj} smaller than this are discouraged.

In addition to these difficulties, there are two other limitations that the user should recognize. First, STAMMT-R is a computationally-intensive code. In particular, the spatial integration after the injection phase must be carried out a very large number of times to obtain convergence in the inverse Laplace-domain algorithm. As such, run-times may be long on some computers. On a 266 MHz Pentium II, runs are generally in excess of 5 minutes. On some computers, runs may exceed 10 mins. As a result, parameter estimation runs may take several hours to complete.

The second limitation is that the code is currently set up to estimate 5 parameters: μ^*, σ, ϕ_f, α_L (two-well), and α_L (SWIW). If another set of estimated parameters is desired, the code must be modified. Modifications must do three things: (1) ensure that the vectors xguess(nx) and xf(nx) are properly modified; (2) ensure that variables transferred by xf(nx) into subroutine obj are still available to obj; and (3) modify output (write) statements to reflect changes. The first change involves changes to xguess(nx) in the main routine only. The second change requires changes to xf(nx) in both the main routine and in the subroutine obj. The third change requires ensuring that if a parameter is removed from storage and transfer in xf(nx) that it becomes available to the subroutine **obj** via a common block. In other words, if a parameter is removed from the estimation, check to ensure that it is brought into obj in a common block. If not, that variable must be brought in within a common block.

7. References

Aitchison, J., and J. A. C. Brown, *The Lognormal Distribution with Special Reference to its Uses in Economics*, Cambridge University Press, New York, 1957.

Ball, W. P., and P. V. Roberts, Long-term sorption of halogenated organic chemicals by aquifer material, 1, Equilibrium, *Environ. Sci. Technol., 25*(7), 1223-1237, 1991a.

Ball, W. P., and P. V. Roberts, Long-term sorption of halogenated organic chemicals by aquifer material, 2, Intraparticle diffusion, *Environ. Sci. Technol., 25*(7), 1237-1249, 1991b.

Brusseau, M. L., R. E. Jessup, and P. S. C. Rao, Modeling the transport of solutes influenced by multiprocess nonequilibrium, *Water Resour. Res., 25*(9), 1971-1988, 1989.

Buchan, G. D., Applicability of the simple lognormal model to particle-size distribution in soils, *Soil Sci., 147*(3), 155-161, 1989.

Buchan, G. D., K. S. Grewal, and A. B. Robson, Improved models of particle-size distribution: An illustration of model comparison techniques, *Soil Sci. Soc. Am. J., 57*(4), 901-908, 1993.

Carrera, J., X. Sánchez-Vila, I. Benet, A. Medina, G. Galarza, and J. Guimerà, On matrix diffusion: Formulations, solution methods and qualitative effects, *Hydrogeol. J., 6*(1), 178-190, 1998.

Chen, C.-S., Analytical and approximate solutions to radial dispersion from an injection well to a geological unit with simultaneous diffusion into adjacent strata, *Water Resour. Res., 21*(8), 1069-1076, 1985.

Chen, C.-S., and G. D. Woodside, Analytical solution for aquifer decontamination by pumping, *Water Resour. Res., 24*(8), 1329-1338, 1988.

Chen, W., and R. J. Wagenet, Solute transport in porous media with sorption-site heterogeneity, *Environ. Sci. Technol., 29*(11), 2725-2734, 1995.

Christian-Frear, T. L., V. C. Tidwell, and L. C. Meigs, *Technical memorandum: results of experimental methodology development for visualizing and quantifying matrix diffusion in the Culebra Dolomite*, Unpublished Report, Milestone number NH184, Sandia National Laboratories, Albuquerque, New Mexico, 1997. The unpublished technical memorandum is on file in the SWCF as WPO#46478.

Connaughton, D. F., J. R. Stedinger, L. W. Lion, and M. L. Shuler, Description of time-varying desorption kinetics: Release of naphthalene from contaminated soils, *Environ. Sci. Technol.*, *27*(12), 2397-2403, 1993.

Cooney, D. O., B. A. Adesanya, and A. L. Hines, Effect of particle size distribution on adsorption kinetics in stirred batch systems, *Chem. Eng. Sci.*, *38*(9), 1535-1541, 1983.

Crank, J., *The Mathematics of Diffusion*, 2nd edition, Oxford University Press, New York, 1975.

Culver, T. B., S. P. Hallisey, D. Sahoo, J. J. Deitsch, and J. A. Smith, Modeling the desorption of organic contaminants from long-term contaminated soil using distributed mass transfer rates, *Environ. Sci. Technol.*, *31*(6), 1581-1588, 1997.

Cunningham, J. A., C. J. Werth, M. Reinhard, and P. V. Roberts, Effects of grain-scale mass transfer on the transport of volatile organics through sediments, 1., Model development, *Water Resour. Res.*, *33*(12), 2713-2726, 1997.

de Hoog, F. R., J. H. Knight, and A. N. Stokes, An improved method for numerical inversion of Laplace transforms, *SIAM J. Sci. Stat. Comput.*, *3*(3), 357-366, 1982.

de Marsily, G., *Quantitative Hydrogeology: Groundwater Hydrology for Engineers*, Academic Press, San Diego, California, 1986.

Dougharty, N. A., Effect of adsorbent particle-size distribution in gas-solid chromatography, *AIChE J.*, *18*(3), 657-659, 1972.

Fong, F. K., and L. A. Mulkey, Solute transport in aggregated media: Aggregate size distribution and mean radii, *Water Resour. Res.*, *26*(6), 1291-1303, 1990.

Grathwohl, P., and S. Kleineidam, Impact of heterogeneous aquifer materials on sorption capacities and sorption dynamics of organic contaminants, In *Groundwater Quality: Remediation and Protection*, Proceedings of the Prague Conference, May 15-18, 1995, K. Kovar, ed., International Association of Hydrological Sciences, Wallingford, Oxfordshire, England, IAHS Publ. no. 225, 79-86, 1995.

Guvanasen, V., and V. M. Guvanasen, An approximate semianalytical solution for tracer injection tests in a confined aquifer with a radially converging flow field and finite volume of tracer and chase fluid, *Water Resour. Res.*, *23*(8), 1607-1619, 1987.

Haggerty, R., *Aquifer Remediation in the Presence of Rate-Limited Mass Transfer*, PhD Dissertation, Stanford University, Stanford, California, 1995.

Haggerty, R., and S. M. Gorelick, Multiple-rate mass transfer for modeling diffusion and surface reactions in media with pore-scale heterogeneity, *Water Resour. Res.*, *31*(10), 2383-2400, 1995.

Haggerty, R., and S. M. Gorelick, Modeling mass transfer processes in soil columns with pore-scale heterogeneity, *Soil Sci. Soc. Am. J.*, *62*(1), 62-74, 1998.

Haggerty, R., and C. F. Harvey, A comparison of estimated mass transfer rate coefficients with the time-scales of the experiments from which they were determined, *Eos Supplement*, *78*(46), F293, 1997.

Harvey, C. F., and S. M. Gorelick, Temporal moment-generating equations: Modeling transport and mass transfer in heterogeneous aquifers, *Water Resour. Res.*, 31(8), 1895-1911, 1995.

Harvey, C. F., R. Haggerty, and S. M. Gorelick, Aquifer remediation: A method for estimating mass transfer rate coefficients and an evaluation of pulsed pumping, *Water Resour. Res.*, *30*(7), 1979-1991, 1994.

Hoeksema, R. J., and P. K. Kitanidis, Analysis of the spatial structure of properties of selected aquifers, *Water Resour. Res., 21*(4), 563-572, 1985.

Kreft, A., and A. Zuber, On the physical meaning of the dispersion equation and its solutions for different initial and boundary conditions, *Chem. Eng. Sci., 33*(11), 1471-1480, 1978.

Lafolie, F., and Ch. Hayot, One-dimensional solute transport modelling in aggregated porous media, Part 1, Model description and numerical solution, *J. Hydrol., 143*(1-2), 63-83, 1993.

Neretnieks, I., and A. Rasmuson, An approach to modelling radionuclide migration in a medium with strongly varying velocity and block sizes along the flow path, *Water Resour. Res., 20*(12), 1823-1836, 1984.

Neuman, S. P., Statistical characterization of aquifer heterogeneities: An overview, In *Recent Trends in Hydrogeology*, T. N. Narasimhan, ed., Spec. Pap. 189, Geol. Soc. Amer., Boulder, Colorado, 81-102, 1982.

Ostensen, R. W., Tracer tests and contaminant transport rates in dual-porosity formations with application to the WIPP, *J. Hydrol., 204*, 197-216, 1998.

Pedit, J. A., and C. T. Miller, Heterogeneous sorption processes in subsurface systems, 1., Model formulations and applications, *Environ. Sci. Technol., 28*(12), 2094-2104, 1994.

Pedit, J. A., and C. T. Miller, Heterogeneous sorption processes in subsurface systems, 2., Diffusion modeling approaches, *Environ. Sci. Technol., 29*(7), 1766-1772, 1995.

Pignatello, J. J., and B. Xing, Mechanisms of slow sorption of organic chemicals to natural particles, *Environ. Sci. Technol., 30*(1), 1-11, 1996.

Rao, P. S. C., R. E. Jessup, and T. M. Addiscott, Experimental and theoretical aspects of solute diffusion in spherical and nonspherical aggregates, *Soil Sci., 133*(6), 342-349, 1982.

Rasmuson, A., The effect of particles of variable size, shape and properties on the dynamics of fixed beds, *Chem. Eng. Sci., 40*(4), 621-629, 1985.

Reeves, M., D. S. Ward, N. D. Johns, and R. M. Cranwell, *Theory and Implementation for SWIFT II, The Sandia Waste-Isolation Flow and Transport Model for Fractured Media*, Release 4.84, Report SAND83-1159, NUREG/CR-3328, Sandia National Laboratories, Albuquerque, New Mexico, 1986.

Satterfield, C. N., C. K. Colton, and W. H. Pitcher Jr., Restricted diffusion in liquids within fine pores, *AIChE J., 19*(3), 628-635, 1973.

Thomas, J. B., *Introduction to Probability*, Springer-Verlag, New York, New York, 1986.

Valocchi, A. J., Use of temporal moment analysis to study reactive solute transport in aggregated porous media, *Geoderma, 46*(1/3), 233-247, 1990.

Villermaux, J., Theory of linear chromatography, In *Percolation Processes, Theory and Applications*, A. E. Rodrigues and D. Tondeur, eds., NATO ASI Series E, vol. 33, Sijthoff and Noordhoff, Rockville, Massachusetts, 83-140, 1981.

Werth, C. J., J. A. Cunningham, P. V. Roberts, and M. Reinhard, Effects of grain-scale mass transfer on the transport of volatile organics through sediments, 2., Column results, *Water Resour. Res., 33*(12), 2727-2740, 1997.

Wu, S-C., and P. M. Gschwend, Numerical modeling of sorption kinetics of organic compounds to soil and sediment particles, *Water Resour. Res., 24*(8), 1373-1383, 1988.

Xu, S., and A. Worman, An investigation of heterogeneity of porosity and diffusivity in cystalline rocks, *Eos Supplement, 78*(46), F330-F331, 1997.

Zlotnik, V. A., and J. D. Logan, Boundary conditions for convergent radial tracer tests and effect of well bore mixing volume, *Water Resour. Res.*, *32*(7), 2323-2328, 1996.

Appendix A1: Parameter Input File for Verification Problem 1

```
1                skipm  !do Multiwell (MW) simulation? 0 if yes, 1 if no
0.0000d0          Tc0   !start time of solute injection (can be 0), MW [T]
0.3000d0         TcE    !elapsed time from t=0 to end of solute inj., MW [T]
0.5083d0         Timein !elapsed time from t=0 to end of chaser inj., MW [T]
0.6588d0         Qin    !injection rate, MW [L^3/T]
0.9720d0         Qout   !pumping rate, MW [L^3/T]
0.4592136D+00    alphLm !longitudinal dispersivity, MW [L]
4.3d0            rmax   !edge of grid for injection, MW [L]
11.0d0           Ro     !distance from injection to pumping wells, MW [L]
0.0602d0         r0i    !well radius (injection, MW) [L]
1                MWtime !use (t,C) input file (set=0) or generate times (set=1), MW
1                MWz    !if MWtime=1: constant time (=0) or ~constant ln(time) (=1) increment, MW
5                MWpumpt!if MWtime=1: elapsed time from Timein to end of pumping [T], MW
50               TNM    !number of time vs concentration data points, MW

0                skips  !do Single Well (SWIW) simulation? 0 if yes, 1 if no
0.1333d0          Tc0s  !start time for solute inj. (can be 0), SWIW [T]
2.25d0           TcEs   !elapsed time from t=0 to end of solute inj., SWIW [T]
6.633d0          Timeins!elapsed time from t=0 to end of chaser inj., SWIW [T]
17.75d0          Trest  !pause length (elapsed time from Timeins to start of pumping), SWIW [T]
0.4665d0         Qins   !injection rate, SWIW [L^3/T]
0.8516d0          Qouts !pumping rate, SWIW [L^3/T]
0.1000D+00        alphLs !longitudinal dispersivity, SWIW [L]
4.0d0            rmaxs  !edge of grid for injection and withdrawal, SWIW [L]
1                SWtime !use (t,C) input file (set=0) or generate times (set=1), SWIW
1                SWz    !if SWtime=1: constant time (=0) or ~constant ln(time) (=1) increment, SWIW
350              SWpumpt!if SWtime=1: elapsed time from (Timeins+Trest) to end of pumping, SWIW [T]
100              TNS    !number of time vs concentration data points, SW

0.098425d0        r0p   !well radius (pumping for MW; injection/withdrawal for SWIW) [L]
7.410d0          b1     !saturated thickness at injection well [L]
7.41d0           b2     !saturated thickness at pumping well [L]
1.d0             Cin    !injection concentration [M/L^3; if Cin=1, conc.'s are effectively normalized and dimensionless]
0.05D-00          poros !advective porosity [-]
0.15D+00         pmat   !diffusive porosity
-6.9077D00        mus   !prescribed (forward) or initial guess (parameter estimation) mus [ln(1/T)]
0.0D+00           sig   !prescribed (forward) or initial guess (parameter estimation) sig
1.0000D+00        Rf    !mobile zone retardation [-]
0.20d0           ptot   !maximum permitted total porosity (inversion parameter) [-]
2.628d-6         Daq    !aqueous diffusion coefficient of solute [L^/T]
0.11             tort   !diffusive tortuosity [-]

1                iest   !0=parameter estimation; 1=forward model only
0                idef   !0=Default distribution; 1 = User-defined distribution
.0d0             disc   !
1000             kmax   !See manual for last 3 parameters; control permissible numerical error, etc.
1.d-5            relerr !
```

Appendix A2: Parameter Input File for Verification Problem 2

```
1               skipm  !do Multiwell (MW) simulation? 0 if yes, 1 if no
0.0000d0        Tc0    !start time of solute injection (can be 0), MW [T]
0.3000d0        TcE    !elapsed time from t=0 to end of solute inj., MW [T]
0.5083d0        Timein !elapsed time from t=0 to end of chaser inj., MW [T]
0.6588d0        Qin    !injection rate, MW [L^3/T]
0.9720d0        Qout   !pumping rate, MW [L^3/T]
0.4592136D+00   alphLm !longitudinal dispersivity, MW [L]
4.3d0           rmax   !edge of grid for injection, MW [L]
11.0d0          Ro     !distance from injection to pumping wells, MW [L]
0.0602d0        r0i    !well radius (injection, MW) [L]
1               MWtime !use (t,C) input file (set=0) or generate times (set=1), MW
1               MWz    !if MWtime=1: constant time (=0) or ~constant ln(time) (=1) increment, MW
5               MWpumpt!if MWtime=1: elapsed time from Timein to end of pumping [T], MW
50              TNM    !number of time vs concentration data points, MW

0               skips  !do Single Well (SWIW) simulation? 0 if yes, 1 if no
0.0d0           Tc0s   !start time for solute inj. (can be 0), SWIW [T]
10.0d0          TcEs   !elapsed time from t=0 to end of solute inj., SWIW [T]
20.00d0         Timeins!elapsed time from t=0 to end of chaser inj., SWIW [T]
1.00d8          Trest  !pause length (elapsed time from Timeins to start of pumping), SWIW [T]
1.0000d0        Qins   !injection rate, SWIW [L^3/T]
10.000d0        Qouts  !pumping rate, SWIW [L^3/T]
0.1000D+00      alphLs !longitudinal dispersivity, SWIW [L]
13.0d0          rmaxs  !edge of grid for injection and withdrawal, SWIW [L]
0               SWtime !use (t,C) input file (set=0) or generate times (set=1), SWIW
0.0             SWz    !if SWtime=1: constant time (=0) or ~constant ln(time) (=1) increment, SWIW
5000.0d0        SWpumpt!if SWtime=1: elapsed time from (Timeins+Trest) to end of pumping, SWIW [T]
299             TNS    !number of time vs concentration data points, SW

0.10d0          r0p    !well radius (pumping for MW; injection/withdrawal for SWIW) [L]
1.00d0          b1     !saturated thickness at injection well [L]
1.00d0          b2     !saturated thickness at pumping well [L]
1.d0            Cin    !injection concentration [M/L^3; if Cin=1, conc.'s are effectively normalized and dimensionless]
0.05D-00        poros  !advective porosity [-]
0.10D+00        pmat   !diffusive porosity
-3.00D00        mus    !prescribed (forward) or initial guess (parameter estimation) mus [ln(1/T)]
3.0D+00         sig    !prescribed (forward) or initial guess (parameter estimation) sig
1.0000D+00      Rf     !mobile zone retardation [-]
0.20d0          ptot   !maximum permitted total porosity (inversion parameter) [-]
2.628d-6        Daq    !aqueous diffusion coefficient of solute [L^/T]
0.11            tort   !diffusive tortuosity [-]

1               iest   !0=parameter estimation; 1=forward model only
0               idef   !0=Default distribution; 1 = User-defined distribution
.0d0            disc   !
1000            kmax   !See manual for last 3 parameters; control permissible numerical error, etc.
1.d-5           relerr !
```

Appendix A3: Parameter Input File for Verification Problem 3

```
0                 skipm  !do Multiwell (MW) simulation? 0 if yes, 1 if no
0.0000d0          Tc0    !start time of solute injection (can be 0), MW [T]
0.3000d0          TcE    !elapsed time from t=0 to end of solute inj., MW [T]
0.5000d0          Timein !elapsed time from t=0 to end of chaser inj., MW [T]
0.5000d0          Qin    !injection rate, MW [L^3/T]
1.0000d0          Qout   !pumping rate, MW [L^3/T]
0.100D+00         alphLm !longitudinal dispersivity, MW [L]
2.0d0             rmax   !edge of grid for injection, MW [L]
10.0d0            Ro     !distance from injection to pumping wells, MW [L]
0.1000d0          r0i    !well radius (injection, MW) [L]
1                 MWtime !use (t,C) input file (set=0) or generate times (set=1), MW
1                 MWz    !if MWtime=1: constant time (=0) or ~constant ln(time) (=1) increment, MW
960               MWpumpt!if MWtime=1: elapsed time from Timein to end of pumping [T], MW
100               TNM    !number of time vs concentration data points, MW

1                 skips  !do Single Well (SWIW) simulation? 0 if yes, 1 if no
0.1333d0          Tc0s   !start time for solute inj. (can be 0), SWIW [T]
2.25d0            TcEs   !elapsed time from t=0 to end of solute inj., SWIW [T]
6.633d0           Timeins!elapsed time from t=0 to end of chaser inj., SWIW [T]
17.75d0           Trest  !pause length (elapsed time from Timeins to start of pumping), SWIW [T]
0.4665d0          Qins   !injection rate, SWIW [L^3/T]
0.8516d0          Qouts  !pumping rate, SWIW [L^3/T]
0.1000D+00        alphLs !longitudinal dispersivity, SWIW [L]
4.0d0             rmaxs  !edge of grid for injection and withdrawal, SWIW [L]
1                 SWtime !use (t,C) input file (set=0) or generate times (set=1), SWIW
1                 SWz    !if SWtime=1: constant time (=0) or ~constant ln(time) (=1) increment, SWIW
350               SWpumpt!if SWtime=1: elapsed time from (Timeins+Trest) to end of pumping, SWIW [T]
100               TNS    !number of time vs concentration data points, SW

0.100000d0        r0p    !well radius (pumping for MW; injection/withdrawal for SWIW) [L]
4.000d0           b1     !saturated thickness at injection well [L]
4.00d0            b2     !saturated thickness at pumping well [L]
1.d0              Cin    !injection concentration [M/L^3; if Cin=1, conc.'s are effectively normalized and dimensionless]
0.01D+00          poros  !advective porosity [-]
0.16D+00          pmat   !diffusive porosity
-6.9078D00        mus    !prescribed (forward) or initial guess (parameter estimation) mus [ln(1/T)]
0.0D+00           sig    !prescribed (forward) or initial guess (parameter estimation) sig
1.0000D+00        Rf     !mobile zone retardation [-]
0.20d0            ptot   !maximum permitted total porosity (inversion parameter) [-]
2.628d-6          Daq    !aqueous diffusion coefficient of solute [L^/T]
0.11              tort   !diffusive tortuosity [-]

1                 iest   !0=parameter estimation; 1=forward model only
0                 idef   !0=Default distribution; 1 = User-defined distribution
.0d0              disc   !
1000              kmax   !See manual for last 3 parameters; control permissible numerical error, etc.
1.d-5             relerr !
```

Appendix A4: Parameter Input Files for Verification Problem 4

1st input parameter file for Verification Problem 4, *QA4A.prm*

```
1                skipm  !do Multiwell (MW) simulation? 0 if yes, 1 if no
0.0000d0         Tc0    !start time of solute injection (can be 0), MW [T]
0.3000d0         TcE    !elapsed time from t=0 to end of solute inj., MW [T]
0.5083d0         Timein !elapsed time from t=0 to end of chaser inj., MW [T]
0.6588d0         Qin    !injection rate, MW [L^3/T]
0.9720d0         Qout   !pumping rate, MW [L^3/T]
0.4592136D+00    alphLm !longitudinal dispersivity, MW [L]
4.3d0            rmax   !edge of grid for injection, MW [L]
11.0d0           Ro     !distance from injection to pumping wells, MW [L]
0.0602d0         r0i    !well radius (injection, MW) [L]
1                MWtime !use (t,C) input file (set=0) or generate times (set=1), MW
1                MWz    !if MWtime=1: constant time (=0) or ~constant ln(time) (=1) increment, MW
5                MWpumpt!if MWtime=1: elapsed time from Timein to end of pumping [T], MW
50               TNM    !number of time vs concentration data points, MW

0                skips  !do Single Well (SWIW) simulation? 0 if yes, 1 if no
0.0000d0         Tc0s   !start time for solute inj. (can be 0), SWIW [T]
2.266667d0       TcEs   !elapsed time from t=0 to end of solute inj., SWIW [T]
6.550d0          Timeins!elapsed time from t=0 to end of chaser inj., SWIW [T]
17.662d0         Trest  !pause length (elapsed time from Timeins to start of pumping), SWIW [T]
0.4392d0         Qins   !injection rate, SWIW [L^3/T]
0.7992d0         Qouts  !pumping rate, SWIW [L^3/T]
0.55342D-01      alphLs !longitudinal dispersivity, SWIW [L]
8.0d0            rmaxs  !edge of grid for injection and withdrawal, SWIW [L]
1                SWtime !use (t,C) input file (set=0) or generate times (set=1), SWIW
0                SWz    !if SWtime=1: constant time (=0) or ~constant ln(time) (=1) increment, SWIW
500              SWpumpt!if SWtime=1: elapsed time from (Timeins+Trest) to end of pumping, SWIW [T]
300              TNS    !number of time vs concentration data points, SW

0.1219d0         r0p    !well radius (pumping for MW; injection/withdrawal for SWIW) [L]
4.400d0          b1     !saturated thickness at injection well [L]
4.400d0          b2     !saturated thickness at pumping well [L]
1.d0             Cin    !injection concentration [M/L^3; if Cin=1, conc.'s are effectively normalized and dimensionless]
0.16342D-02      poros  !advective porosity [-]
0.16D+00         pmat   !diffusive porosity
-7.6887D00       mus    !prescribed (forward) or initial guess (parameter estimation) mus [ln(1/T)]
3.5654D+00       sig    !prescribed (forward) or initial guess (parameter estimation) sig
1.0000D+00       Rf     !mobile zone retardation [-]
0.35d0           ptot   !maximum permitted total porosity (inversion parameter) [-]
2.628d-6         Daq    !aqueous diffusion coefficient of solute [L^/T]
0.11             tort   !diffusive tortuosity [-]

1                iest   !0=parameter estimation; 1=forward model only
0                idef   !0=Default distribution; 1 = User-defined distribution
.0d0             disc   !
1000             kmax   !See manual for last 3 parameters; control permissible numerical error, etc.
1.d-5            relerr !
```

2nd input file for Verification Problem 4, *QA4B.dst*

0.19714D-09	0.85961D-03
0.45124D-09	0.15047D-02
0.10329D-08	0.38137D-02
0.23642D-08	0.91623D-02
0.54114D-08	0.20866D-01
0.12386D-07	0.45050D-01
0.28352D-07	0.92209D-01
0.64896D-07	0.17894D+00
0.14854D-06	0.32927D+00
0.34000D-06	0.57454D+00
0.77825D-06	0.95076D+00
0.17814D-05	0.14923D+01
0.40774D-05	0.22222D+01
0.93329D-05	0.31398D+01
0.21362D-04	0.42104D+01
0.48897D-04	0.53603D+01
0.11192D-03	0.64812D+01
0.25618D-03	0.74458D+01
0.58639D-03	0.81323D+01
0.13422D-02	0.84498D+01
0.30722D-02	0.83598D+01
0.70322D-02	0.78835D+01
0.16096D-01	0.70958D+01
0.36843D-01	0.61060D+01
0.84332D-01	0.50336D+01
0.19303D+00	0.39851D+01
0.44183D+00	0.30393D+01
0.10113D+01	0.22409D+01
0.23149D+01	0.16039D+01
0.52986D+01	0.11196D+01
0.12128D+02	0.76594D+00
0.27760D+02	0.51604D+00
0.63542D+02	0.34391D+00
0.14544D+03	0.22754D+00
0.33291D+03	0.44513D+00

3rd input parameter file for Validation Problem 4, *QA4B.prm*

```
1               skipm  !do Multiwell (MW) simulation? 0 if yes, 1 if no
0.0000d0        Tc0    !start time of solute injection (can be 0), MW [T]
0.3000d0        TcE    !elapsed time from t=0 to end of solute inj., MW [T]
0.5083d0        Timein !elapsed time from t=0 to end of chaser inj., MW [T]
0.6588d0        Qin    !injection rate, MW [L^3/T]
0.9720d0        Qout   !pumping rate, MW [L^3/T]
0.4592136D+00   alphLm !longitudinal dispersivity, MW [L]
4.3d0           rmax   !edge of grid for injection, MW [L]
11.0d0          Ro     !distance from injection to pumping wells, MW [L]
0.0602d0        r0i    !well radius (injection, MW) [L]
1               MWtime !use (t,C) input file (set=0) or generate times (set=1), MW
1               MWz    !if MWtime=1: constant time (=0) or ~constant ln(time) (=1) increment, MW
5               MWpumpt!if MWtime=1: elapsed time from Timein to end of pumping [T], MW
50              TNM    !number of time vs concentration data points, MW

0               skips  !do Single Well (SWIW) simulation? 0 if yes, 1 if no
0.0000d0        Tc0s   !start time for solute inj. (can be 0), SWIW [T]
2.266667d0      TcEs   !elapsed time from t=0 to end of solute inj., SWIW [T]
6.550d0         Timeins!elapsed time from t=0 to end of chaser inj., SWIW [T]
17.662d0        Trest  !pause length (elapsed time from Timeins to start of pumping), SWIW [T]
0.4392d0        Qins   !injection rate, SWIW [L^3/T]
0.7992d0        Qouts  !pumping rate, SWIW [L^3/T]
0.55342D-01     alphLs !longitudinal dispersivity, SWIW [L]
8.0d0           rmaxs  !edge of grid for injection and withdrawal, SWIW [L]
1               SWtime !use (t,C) input file (set=0) or generate times (set=1), SWIW
0               SWz    !if SWtime=1: constant time (=0) or ~constant ln(time) (=1) increment, SWIW
500             SWpumpt!if SWtime=1: elapsed time from (Timeins+Trest) to end of pumping, SWIW [T]
300             TNS    !number of time vs concentration data points, SW

0.1219d0        r0p    !well radius (pumping for MW; injection/withdrawal for SWIW) [L]
4.400d0         b1     !saturated thickness at injection well [L]
4.400d0         b2     !saturated thickness at pumping well [L]
1.d0            Cin    !injection concentration [M/L^3; if Cin=1, conc.'s are effectively normalized and dimensionless]
0.16342D-02     poros  !advective porosity [-]
0.16D+00        pmat   !diffusive porosity
-7.6887D00      mus    !prescribed (forward) or initial guess (parameter estimation) mus [ln(1/T)]
3.5654D+00      sig    !prescribed (forward) or initial guess (parameter estimation) sig
1.0000D+00      Rf     !mobile zone retardation [-]
0.35d0          ptot   !maximum permitted total porosity (inversion parameter) [-]
2.628d-6        Daq    !aqueous diffusion coefficient of solute [L^/T]
0.11            tort   !diffusive tortuosity [-]

1               iest   !0=parameter estimation; 1=forward model only
1               idef   !0=Default distribution; 1 = User-defined distribution
.0d0            disc   !
1000            kmax   !See manual for last 3 parameters; control permissible numerical error, etc.
1.d-5           relerr !
```

Distribution
SAND99-0164

Federal Agencies

US Department of Energy (4)
Office of Civilian Radioactive Waste Mgmt.
Attn: Deputy Director, RW-2
Acting Director, RW-10
Office of Human Resources & Admin.
Director, RW-30
Office of Program Mgmt. & Integ.
Director, RW-40
Office of Waste Accept., Stor., & Tran.
Forrestal Building
Washington, DC 20585

Yucca Mountain Site Characterization Office
Director, RW-3
Office of Quality Assurance
Attn: Project Director
P. O. Box 30307
Las Vegas, NV 89036-0307

US Department of Energy
Research & Waste Management Division
Attn: Director
P.O. Box E
Oak Ridge, TN 37831

US Department of Energy (6)
Carlsbad Area Office
Attn: I. Triay
G. T. Basabilvazo
D. Galbraith
M. McFadden
J. A. Mewhinney
D. Mercer
Mailroom
P.O. Box 3090
Carlsbad, NM 88221-3090

US Department of Energy
Office of Environmental Restoration and
Waste Management
Attn: M. Frei, EM-30
Forrestal Building
Washington, DC 20585-0002

US Department of Energy (3)
Office of Environmental Restoration and
Waste Management
Attn: J. Juri, EM-34, Trevion II
Washington, DC 20585-0002

US Department of Energy
Office of Environmental Restoration and
Waste Management
Attn: S. Schneider, EM-342, Trevion II
Washington, DC 20585-0002

US Department of Energy (2)
Office of Environment, Safety & Health
Attn: C. Borgstrom, EH-25
R. Pelletier, EH-231
Washington, DC 20585

US Department of Energy (2)
Idaho Operations Office
Fuel Processing & Waste Mgmt. Division
785 DOE Place
Idaho Falls, ID 83402

US Environmental Protection Agency (2)
Radiation Protection Programs
Attn: M. Oge
ANR-460
Washington, DC 20460

Boards

Defense Nuclear Facilities Safety Board
Attn: D. Winters
625 Indiana Ave. NW, Suite 700
Washington, DC 20004

Nuclear Waste Technical Review Board (2)
Attn: Chairman
J. L. Cohon
2300 Clarendon Blvd. Ste 1300
Arlington, VA 22201-3367

State Agencies

Attorney General of New Mexico
P.O. Drawer 1508
Santa Fe, NM 87504-1508

Environmental Evaluation Group (3)
Attn: Library
7007 Wyoming NE
Suite F-2
Albuquerque, NM 87109

NM Environment Department (3)
Secretary of the Environment
1190 St. Francis Drive
Santa Fe, NM 87503-0968

NM Bureau of Mines & Mineral Resources
Socorro, NM 87801

Laboratories/Corporations

Battelle Pacific Northwest Laboratories
Battelle Blvd.
Richland, WA 99352

Los Alamos National Laboratory
Attn: B. Erdal, INC-12
P.O. Box 1663
Los Alamos, NM 87544

Tech Reps, Inc. (3)
Attn: J. Chapman (1)
Loretta Robledo (2)
5000 Marble NE, Suite 222
Albuquerque, NM 87110

Westinghouse Electric Corporation (5)
Attn: Library
J. Epstein
J. Lee
R. Kehrman
P.O. Box 2078
Carlsbad, NM 88221

S. Cohen & Associates
Attn: Bill Thurber
1355 Beverly Road
McLean, VA 22101

Sean Fleming
Waterstone Environmental Hydrology and Engineering
1650 38th Street, Suite 201E
Boulder, Colorado 80301

Michael Gross
415 Riviera Drive
San Rafael, CA 94901-1530

National Academy of Sciences WIPP Panel

Tom Kiess (15)
Staff Study Director
GF456
2101 Constitution Ave.
Washington, DC 20418

Universities

University of New Mexico
Geology Department
Attn: Library
141 Northrop Hall
Albuquerque, NM 87131

University of Washington
College of Ocean & Fishery Sciences
Attn: G. R. Heath
583 Henderson Hall, HN-15
Seattle, WA 98195

Roy Haggerty (5)
Dept. of Geosciences
104 Wilkinson Hall
Oregon State University
Corvallis, OR 97331-5506

Libraries

Thomas Brannigan Library
Attn: D. Dresp
106 W. Hadley St.
Las Cruces, NM 88001

Government Publications Department
Zimmerman Library
University of New Mexico
Albuquerque, NM 87131

New Mexico Junior College
Pannell Library
Attn: R. Hill
Lovington Highway
Hobbs, NM 88240

New Mexico State Library
Attn: N. McCallan
325 Don Gaspar
Santa Fe, NM 87503

New Mexico Tech
Martin Speere Memorial Library
Campus Street
Socorro, NM 87810

WIPP Information Center
Attn: Y. Acosta
4021 National Parks Highway
Carlsbad, NM 88220

Foreign Addresses

Atomic Energy of Canada, Ltd.
Whiteshell Laboratories
Attn: B. Goodwin
Pinawa, Manitoba, CANADA R0E 1L0

Francois Chenevier (2)
ANDRA
Parc de la Croix Blanche
1-7 rue Jean Monnet
92298 Chatenay-Malabry Cedex
FRANCE

Claude Sombret
Centre d'Etudes Nucleaires de la Vallee Rhone
CEN/VALRHO
S.D.H.A. B.P. 171
30205 Bagnols-Sur-Ceze
FRANCE

Commissariat a L'Energie Atomique
Attn: D. Alexandre
Centre d'Etudes de Cadarache
13108 Saint Paul Lez Durance Cedex
FRANCE

Bundesanstalt fur Geowissenschaften und
Rohstoffe
Attn: M. Langer
Postfach 510 153
D-30631 Hannover
GERMANY

Bundesministerium fur Forschung und
Technologie
Postfach 200 706
5300 Bonn 2
GERMANY

Gesellschaft fur Anlagen und Reaktorsicherheit
(GRS)
Attn: B. Baltes
Schwertnergasse 1
D-50667 Cologne
GERMANY

Dr.-Ing. Klaus Kuhn
TU Clausthal Institut fur Bergbau
Erzstr. 20
D-38678 Clausthal-Zellerfeld
GERMANY

Shingo Tashiro
Japan Atomic Energy Research Institute
Tokai-Mura, Ibaraki-Ken, 319-11
JAPAN

Netherlands Energy Research Foundation ECN
Attn: J. Prij
3 Westerduinweg
P.O. Box 1
1755 ZG Petten
THE NETHERLANDS

Svensk Karnbransleforsorjning AB
Attn: F. Karlsson
Project KBS (Karnbranslesakerhet)
Box 5864
S-102 48 Stockholm
SWEDEN

Nationale Genossenschaft fur die Lagerung
Radioaktiver Abfalle (2)
Attn: S. Vomvoris
P. Zuidema
Hardstrasse 73
CH-5430 Wettingen
SWITZERLAND

AEA Technology
Attn: J. H. Rees
D5W/29 Culham Laboratory
Abington, Oxfordshire OX14 3DB
UNITED KINGDOM

AEA Technology
Attn: W. R. Rodwell
044/A31 Winfrith Technical Centre
Dorchester, Dorset DT2 8DH
UNITED KINGDOM

AEA Technology
Attn: J. E. Tinson
B4244 Harwell Laboratory
Didcot, Oxfordshire OX11 ORA
UNITED KINGDOM

Internal

MS	Org.	
0701	6100	L. Shephard
0701	6100	P. B. Davies
0779	6849	D. R. Anderson
0779	6848	H. N. Jow
0771	6800	M. Chu
0733	6832	J. T. Holmes
0735	6115	S. J. Altman
1395	6821	R. L. Beauheim
1395	6821	C. Bryan
0735	6115	R. M. Holt
0735	6115	M. Kelley
1395	6821	M. K. Knowles
0735	6115	S. A. McKenna
0735	6115	L. C. Meigs

0733	6832	H. W. Papenguth
1395	6821	G. W. Perkins
0735	6115	P. C. Reeves
1395	6821	R. M. Roberts
0735	6115	E. K. Webb
1395	6821	M. Marietta
1395	6810	N. Z. Elkins
1395	6860	R. D. Waters
0731	6811	C. Northrop-Salazar (2)
0731	6811	NWM Library (20)
9018	8940-2	Central Technical Files
0899	4916	Technical Library (2)
0612	4912	Review and Approval Desk, For DOE/OSTI